PCCP

Accepted Manuscript

This is an *Accepted Manuscript*, which has been through the Royal Society of Chemistry peer review process and has been accepted for publication.

Accepted Manuscripts are published online shortly after acceptance, before technical editing, formatting and proof reading. Using this free service, authors can make their results available to the community, in citable form, before we publish the edited article. We will replace this *Accepted Manuscript* with the edited and formatted *Advance Article* as soon as it is available.

You can find more information about *Accepted Manuscripts* in the **Information for Authors**.

Ion-Pair Formation in Aqueous Strontium Chloride and Strontium Hydroxide Solutions under Hydrothermal Conditions by AC Conductivity Measurements

H. Arcis[†], G. H. Zimmerman[*,‡] and P. R. Tremaine[*,†]

[†]Department of Chemistry, University of Guelph, Guelph, Ontario, CanadaN1G 2W1

[‡]Department of Chemistry and Biochemistry, Bloomsburg University, Bloomsburg, Pennsylvania17815, United States

E-mail address:[†] harcis@uoguelph.ca,[†] tremaine@uoguelph.ca, [‡]gzimmerm@bloomu.edu

ABSTRACT

Frequency-dependent electrical conductivities of solutions of aqueous strontium hydroxide and strontium chloride have been measured from $T = 295$ K to $T = 625$ K at $p = 20$ MPa, over a very wide range of ionic strength, ($3 \cdot 10^{-5}$ to 0.2 mol·kg^{-1}) using a high-precision flow AC conductivity instrument. Experimental values for the concentration-dependent equivalent conductivity, Λ, of the two electrolytes were fitted with the Turq-Blum-Bernard-Kunz ("TBBK") ionic conductivity model, to determine ionic association constants, $K_{A,m}$. The TBBK fits yielded statistically significant formation constants for the species SrOH$^+$ and SrCl$^+$ at all temperatures, and for Sr(OH)$_2{}^0$ and SrCl$_2{}^0$ at temperatures above 446 K. The first and second stepwise association constants for the ion pairs followed the order K_{A1} (SrOH$^+$) $>K_{A1}$(SrCl$^+$) $>K_{A2}$[Sr(OH)$_2{}^0$] $>K_{A2}$[SrCl$_2{}^0$], consistent with long-range solvent polarization effects associated with the lower static dielectric constant and high compressibility of water at elevated temperatures. The stepwise association constants to form SrCl$^+$ agree with previously reported values for CaCl$^+$ to within the combined experimental error at high temperatures and, at temperatures below ~375 K, the values of $\log_{10} K_{A1}$ for strontium are lower than those for calcium by up to ~ 0.3-0.4 units. The association constants for the species SrOH$^+$ and Sr(OH)$_2{}^0$ are the first accurate values to be reported for hydroxide ion pairs with any divalent cation under these conditions.

KEYWORDS: conductivity, hydrothermal solution, ion association, strontium chloride, strontium hydroxide, hydrolysis, TBBK.

1. Introduction

During the past four decades, there been major advances in our understanding of the physical chemistry of simple ions and non-electrolytes in high temperature water, based on quantitative thermodynamic and transport property measurements and spectroscopic studies with new experimental tools designed to operate under the harsh corrosive conditions that exist under hydrothermal conditions.[1, 2] Semi-empirical "equations of state" to describe the standard partial molar properties of aqueous species have now been formulated,[3,4] and these have widespread use for applications to inorganic and organic geochemistry, marine chemistry, and industrial process design. There are two serious deficiencies in the database from which these models were derived. The first is that most of the experimental measurements on which these models are based are restricted to temperatures below 573 K. The temperature range from 573 up to and above the critical point of water at 673 K and 22 MPa remains relatively unexplored. This presents a major opportunity for frontier research if suitable quantitative measurement techniques can be developed. The challenges are formidable, because the conditions are extremely aggressive; ion association is extensive but not complete; and solubilities can be very low.[2,5] The second deficiency is that the database for the ion pairs and coordination complexes of aqueous cations at temperatures above ~ 400 K is extremely limited. The hydrothermal literature for metal complexes with inorganic and organic ligands has been reviewed by Sverjensky at al.,[6] Shock and Koretsky,[7] and in recent IAPWS publications.[1,8] The low solubilities of many salts at elevated temperature prevents the application of most spectroscopic techniques. As a result, experimental values for formation constants under hydrothermal conditions have largely been determined from ligand-concentration dependent UV-visible spectra, solubility measurements, and a small number of potentiometric studies. High temperature data are limited and most of the values in geochemical and industrial databases for hydrothermal conditions come from extrapolations and correlations based on measurements below 300 K. Despite their importance, the experimental databases for hydroxy-complexes are even more limited. With only a few exceptions, hydrolysis constants for most metals must be determined from pH-dependent solubility studies.[9-11] The measurement of equilibrium pH and

sampling of dissolved metals at sub-µmolal concentrations pose serious challenges, and there are large uncertainties in almost all of the "best" experimental values.[9] Most of the values in the widely used compilation by Shock et al.[11] are derived from correlations based on data for oxy-anions, which are structural different from hydroxy-complexes, or extrapolations of values below 300 K.

The association constants of hydroxide with strontium are especially important in this context, because the solid, $Sr(OH)_2(s)$, is moderately soluble in near-critical water. It is thus more amenable to accurate experimental studies, and has the potential to be used as a model system for other alkaline earth and metal M^{2+} species. The association of the chloride ion with mono- and divalent cations under hydrothermal conditions has received more study,[1,6] however accurate equilibrium constants are known for only a few systems. Moreover, strontium ion is an important fission product in nuclear reactors which operate with very tightly controlled coolant pH. It is also a major component of naturally occurring radioactive material ("NORM") scales, which form in oilfield production systems at these temperatures. There is a need to model the chemistry in both of these energy production applications. No experimental values for the association constants of aqueous strontium hydroxide or aqueous strontium chloride under hydrothermal conditions have been reported in the literature.

Although conductivity techniques for measuring ionic association at high temperatures and pressure have been available for many years, the development of flow AC conductance instruments by R.H. Wood and his group has provided a new tool for measuring the limiting ionic conductivities and ion-pair formation constants of very dilute solutions under extreme conditions.[12,13] This paper reports the results of a study to determine the association constants of strontium hydroxide and strontium chloride, under conditions approaching the critical point of water, using a modified state-of-the-art, high-temperature, flow AC conductance instrument originally built at the University of Delaware.[12,14,15] Measurements were carried out using a series of solutions at concentrations as low as 10^{-5} mol·L^{-1}, at temperatures from 295 K up to 625 K at a constant applied pressure of ~20 MPa. The first part of this study[16] examined the properties of sodium and strontium triflate in the same series of experimental runs, to determine values for the limiting conductivity of the Sr^{2+} ion required to interpret these results. The

present paper reports the second and major part of this study, which yielded first and second stepwise association constants of strontium hydroxide and strontium chloride, $K_{A,1}$ and $K_{A,2}$, under these very challenging and aggressive conditions.   The results are compared to the very limited experimental database for other M^{2+} hydroxide and chloride ion pairs, to the extrapolated values from estimated standard partial molar properties and molecular simulations, and to the results of molecular simulations.

2. Experimental

2.1   Chemicals and Solution Preparation

Two aqueous stock solutions of strontium chloride of accurate composition within ± 0.1% (approximately 0.4 and 0.2 m / mol·kg^{-1}) were prepared from $SrCl_2$(s) purchased from Alfa Aesar (99.5% anhydrous metals basis, Lot# D20U031 and Lot# B18W022 respectively). After mixing the salt with pure water, a small amount of grey particulate matter formed, believed to be strontium carbonate, which was removed by filtration. Both solutions were analyzed gravimetrically by water evaporation[17] in triplicate with a precision of 0.01%. The former solution was used to prepared dilute solutions from $T = 295$ to 600 K while the later one was only used at $T = 625$ K.

Three aqueous stock solutions of strontium hydroxide of accurate composition within ± 0.1% (approximately 0.03 m) were prepared from $Sr(OH)_2 \cdot 8H_2O$(s) purchased from Alfa Aesar (99% metals basis, Lot# G16U029). Solutions were filtered and put into a polyethylene bottle under an argon flow. Solutions were analyzed by mass titration with potassium hydrogen phthalate in triplicate with a precision of 0.01%. Solutions were always stored in a desiccator under an argon atmosphere. The first solution was used at $T = 295$, the second from $T = 375$ to 448 K and the third for $T > 448$ K.

The conductivity cell constant was determined using KCl solutions, identical to those used in our previous study.[16] The solutions were prepared by mass from crystalline KCl purchased from Alfa Aesar (99.995 % metals basis, Lot # E21U0) and dried at 573 K to constant mass of 0.01%.

All solutions described above were prepared using degassed and deionized water from a Millipore Direct-Q 5 water purification system (resistivity 18.2 MΩ·cm) with buoyancy corrections for preparations by mass.

Solutions measured in the conductance instrument were prepared by mass dilution under argon from the stock solutions in sealed Pyrex bottles for $SrCl_2$ and KCl, and in sealed high-density polyethylene bottles (Nalgene[®]) for $Sr(OH)_2$). They were then pumped from these same bottles directly into the conductivity cell using the procedures described below.

2.2   AC Conductivity Flow Cell and Injection System

Conductivity experiments were performed using a high-temperature, high-pressure conductivity flow cell, described in detail elsewhere.[16,18]   Briefly, the cell consists of a long platinum inlet tube that leads into a platinized cup which forms the outer electrode. The inner electrode is a platinum rod that has been electrodeposited with platinum black and is a direct extension of the platinum outlet tube which carries the exiting solution away from the cell. The electrodes are separated from one-another by a system of sapphire and ceramic insulators, located downstream of the cell, and contained in a titanium cell body which compresses annealed gold discs to provide a pressure seal. A diamond frit positioned at the cell exit prevents the backflow of impurities from the sapphire.   The temperatures of the cell, its surrounding oven, and the inlet tube were controlled using three independent systems, capable of regulating to ± 0.15 K over several hours, and measured to ± 0.02 K with a platinum resistance thermometer. High-performance liquid chromatographic (HPLC) pumps were used to inject solutions into the flow conductivity cell, at a rate of 0.5 $cm^3 \cdot min^{-1}$.   The pressure was controlled by a back-pressure regulator located at the end of the flow line, and measured to an accuracy of ± 0.01 MPa.

The experimental design is based on that of our previous study,[16] which requires the sequential determination of the conductivities of aqueous solutions of $Sr(OH)_2$ and $SrCl_2$ as a function of concentration at the same temperature, pressure and flow rate. To minimize solvent corrections,

solutions of each solute at increasing concentrations were prepared in the same bottle, by injecting increments of stock solution from a weighed syringe through a septum into the solution.   This permits the most accurate measurement of the conductivity of the pure solvent and, because each subsequent solution is more concentrated, minimizes contamination due to solute adsorption to the cell walls. A very wide range of concentration (10^{-5} to 0.2 mol·kg^{-1}) was used for $SrCl_2$ to ensure that association effects could be measured accurately. A slightly more restricted range (10^{-5} to 0.03 mol·kg^{-1}) was used for $Sr(OH)_2$ to avoid precipitating $Sr(OH)_2(s)$. At $T = 600$ K and 625 K the maximum concentration $1 \cdot 10^{-2}$ and $4 \cdot 10^{-3}$ mol·kg^{-1}, respectively because higher concentrations caused the inlet line to plug. The solution preparation procedure was repeated at each temperature.

A programmable automatic RCL meter (Fluke Model PM6304C) was used to measure the angular frequency (ω) dependence of the solution complex impedance, $Z(\omega) = Z_{Re}(\omega) - j \cdot Z_{Im}(\omega)$, where , $j^2 = -1$. Both real $Z_{Re}(\omega)$ and imaginary $Z_{Im}(\omega)$ components of the impedance spectrum were obtained at frequencies, $f = \omega/2\pi$, of 100, 200, 500, 1000, 2000, 5000, 10000, 20000, 100000 Hz. Eighty to one hundred measurements were taken with a computer over a time span 50 minutes or more. Details of the frequency-dependent measurements and the experimental uncertainty limits in $Z_{Re}(\omega)$ and $Z_{Im}(\omega)$ are discussed in References 16, 18-22. Our previous studies,[16,18,22] showed that, for our type of cell, an extrapolation of $Z_{Re}(\omega)$, according to the expression:

$$Z_{Re}(\omega) = R_s + b_1 \cdot \omega^{-n},$$

(1)

yielded the most accurate results for concentrated electrolyte solutions. Here R_s is the solution resistance that we report; b_1, and the exponential term n are fitting parameters.[15]

3. Results

3.1 Experimental Conductivities.

Experimental conductivities of aqueous solutions of $SrCl_2$ and $Sr(OH)_2$ were obtained in the same course of measurements as those on $NaCF_3SO_3$ and $Sr(CF_3SO_3)_2$ that formed the first part of this study.[16] The procedures used for calibrating the instruments and determining the cell constants are reported in Ref. 16.   The experimental conductivities of the electrolyte solutions, κ_{soln}^{exp}, were corrected for impurities within the solvent and the self ionization of water by subtracting the experimental values for H_2O, κ_w^{exp}, for each run, using the method of Sharygin et al.:[23]

$$\kappa = \kappa_{soln}^{exp} - \kappa_w^{exp} \quad , \tag{2}$$

where the conductivities κ, κ_{soln}^{exp} and κ_w^{exp} are in SI units of $S \cdot m^{-1}$. In this study, these were converted to units of $S \cdot cm^{-1}$.

Theoretical conductivity equations make use of the equivalent conductivity of the solution, Λ^{exp}, which is defined as follows:

$$\Lambda^{exp} = \frac{\kappa}{N} \tag{3}$$

Here, N is the normality or equivalent concentration in $moleq \cdot L^{-1}$, giving the expression:

$$N = \sum c_M^c z_M^c = \sum c_X^a \left| z_X^a \right| \quad , \tag{4}$$

where c_M^c, c_X^a and z_M^c, z_X^a are the molarities and the charge of the cations M^{z+} and the anions X^{z-}, respectively. Molarities, c_i, and molalities, m_i, are related by the expression,

$$c_i = \frac{1000 \cdot m_i \cdot \rho_s}{m_i \cdot M_i + 1000} \tag{5}$$

where M_i is the molar mass of the species i; and ρ_s is the density of the solution.

The calculation of equivalent conductivities, Λ^{exp}, from eqs 3-5, requires the conversion of molalities, m, to concentrations, c. This calculation requires accurate solution densities. For dilute solutions this may be done by assuming that the density of the solution is equal to that of pure water, for which accurate pVT data formulations are known.[24] However, at the high concentrations used in this study the densities deviate substantially from those of pure liquid water at temperatures above ~570 K.[25] No data regarding the densities of aqueous $Sr(OH)_2$ or $SrCl_2$ have been reported in the literature under these conditions. As in our previous studies,[16,18] we addressed this issue by using the Helgeson-Kirkham-Flowers-Tanger ("HKF") model to estimate the standard partial molar volumes $V°$ of the aqueous ions and ion-pairs in our solutions.[6,7,26,27] The calculation required knowledge of solution speciation, which we determined in an iterative process by fitting the TBBK model to our experimental conductivity data, using procedures presented below in Section 3. The method, and its accuracy, are discussed in Ref. 16. Values of the HKF parameters for the strontium species, were estimated using the assumptions $V°[Sr(OH)_2{}^0] = V°[CaCl_2{}^0]$; and $V°[SrCl_2{}^0] = V°[CaCl_2{}^0]$.[6]

The concentrations and the corresponding experimental equivalent conductivities, Λ^{exp}, at each molality of aqueous $SrCl_2$ and $Sr(OH)_2$ are tabulated in Tables 1 and 2, along with the average temperature (IPTS-90) and pressure. The equivalent conductivities are plotted against molarity, expressed as $c^{1/2}$, in Figures 1 and 2. The uncertainties in Tables 1 and 2 were estimated using the procedures identical to those reported in our previous study.[16] A comparison of the equivalent conductivities of $Sr(OH)_2$ and $SrCl_2$ at 625 K and 20 MPa is plotted in Figure 3.

3.2   **Data Treatment with the Turq-Blum-Bernard-Kunz ("TBBK") Conductivity Model**

The Turq-Blum-Bernard-Kunz ("TBBK") conductivity model,[28] was used to treat all of the experimental equivalent conductivity measurements in this work. The procedures are described in our previous study on sodium and strontium triflate.[16]

In dilute aqueous solutions and at low temperature, strontium chloride and strontium hydroxide are known to be fully dissociated. However, as solutions become more concentrated and temperature increases up to hydrothermal conditions Sr^{2+}, Cl^- and OH^- can associate to form a charged ion-pair, $Sr(Cl)^+_{(aq)}$, $Sr(OH)^+_{(aq)}$, or a triplet ion $Sr(Cl)^0_{2\,(aq)}$, $Sr(OH)^0_{2\,(aq)}$ according to the following equilibria:

$$Sr^{2+}_{(aq)} + OH^-_{(aq)} \leftrightharpoons Sr\left(OH\right)^+_{(aq)} \qquad\qquad K_{A_1,Sr(OH)^+} = \frac{a_{Sr(OH)^+}}{a_{Sr^{2+}} \cdot a_{OH^-}} \qquad (6)$$

$$Sr^{2+}_{(aq)} + Cl^-_{(aq)} \leftrightharpoons SrCl^+_{(aq)} \qquad\qquad K_{A_1,SrCl^+} = \frac{a_{SrCl^+}}{a_{Sr^{2+}} \cdot a_{Cl^-}} \qquad (7)$$

$$Sr\left(OH\right)^+_{(aq)} + OH^-_{(aq)} \leftrightharpoons Sr\left(OH\right)^0_{2\,(aq)} \qquad\qquad K_{A_2,Sr(OH)^0_2} = \frac{a_{Sr(OH)^0_2}}{a_{Sr(OH)^+} \cdot a_{OH^-}} \qquad (8)$$

$$SrCl^+_{(aq)} + Cl^-_{(aq)} \leftrightharpoons SrCl^0_{2\,(aq)} \qquad\qquad K_{A_2,SrCl^0_2} = \frac{a_{SrCl^0_2}}{a_{SrCl^+} \cdot a_{Cl^-}} \qquad (9)$$
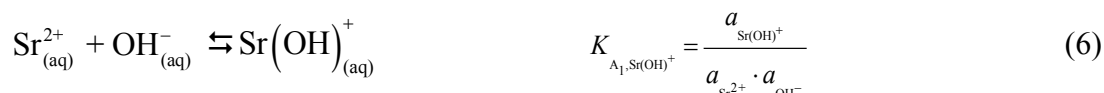
As in our earlier study,[16] the TBBK treatment of the strontium systems is based on the equations from the original paper,[28] corrected to address important misprints found by other authors.[23,29] The activity coefficients of the ionic species in this model are derived from the corresponding MSA expression.[28,30] Following Sharygin et al.,[23] the Bjerrum distance was used in the coulombic contribution and

crystallographic radii for the hard sphere contribution. For all neutral species, the activity coefficients were set equal to 1. As in our previous study,[16] in order to define the theoretical conductivity, κ, we used the mixing rule recommended by Sharygin et al.,[23] based on a critical evaluation of several modern treatments.

In our calculations, the properties of water (density, ρ_w; viscosity, η_w; and static dielectric constant, ε_w) were determined from the equations of state reported by Wagner and Pruss,[24] Huber et al.,[31] and Fernandez et al.,[32] respectively. Values for the ionization constant of water, K_w, (eq 10) were calculated from Bandura and Lvov:[33]

$$\text{H}_2\text{O} \leftrightharpoons \text{H}^+_{(aq)} + \text{OH}^-_{(aq)} \qquad\qquad K_w = \frac{a_{\text{H}^+} \cdot a_{\text{OH}^-}}{a_{\text{H}_2\text{O}}} \qquad\qquad (10)$$

The TBBK model also requires the ionic radii and limiting conductivities of the species at T, p. The radii of single ions were set equal to the crystallographic radii compiled by Marcus.[34] The radii of the ion pairs were calculated from the cube-root expressions used by Wood and his co-workers:[14,15,35]

$$r_{\text{SrX}^+} = \left(r^3_{\text{Sr}^{2+}} + r^3_{\text{X}^-} \right)^{1/3} \qquad\qquad (11)$$

$$r_{\text{Sr}(\text{X}_2)^0_2} = \left(r^3_{\text{Sr}^{2+}} + 2 \cdot r^3_{\text{X}^-} \right)^{1/3} \qquad\qquad (12)$$

where X^- stands for $(\text{OH})^-$ or Cl^-.

In order to use the TBBK equation, an accurate estimate of the ionic equivalent conductivity for Sr^{2+} was needed. Our treatment is based on the experimental values of $\lambda°(\text{Sr}^{2+})$ measured in our study of strontium triflate.[16] The fitted parameters for the reduced density relationship of Marshall,[36] reported in

Ref. 16 were used to calculate $\lambda°(Sr^{2+})$, at the desired temperature and pressure. The values for the limiting equivalent conductivity for H^+ and OH^- at infinite dilution were taken from Marshall,[36] except those for OH^- at temperatures above 300 K, which were taken from Ho et al.[37] The limiting equivalent conductivities at infinite dilution for the $SrCl^+$ and $Sr(OH)^+$ ion pairs were estimated from the expression reported by Anderko and Lencka:[5]

$$\lambda°_{\text{ion pair}} = \frac{\left|z_{\text{ion pair}}\right|}{\left[\sum_{i=1}^{n}\left(\frac{z_i}{\lambda°_i}\right)^3\right]^{1/3}} ,$$

(13)

where z is the charge of the ion or ion pair. This method agreed well with the results of Bianchi et al.[38] for the $MgCl^+$ ion pair. The resulting values for $\lambda°(Sr^{2+})$, $\lambda°(Cl^-)$, $\lambda°(OH^-)$, $\lambda°(H^+)$, $\lambda°(SrCl^+)$ and $\lambda°(SrOH^+)$, at each set of experimental conditions, are given in Tables 3 and 4. The sums of $\lambda°(Sr^{2+})$ + $\lambda°(Cl^-)$, and of $\lambda°(Sr^{2+})$ + $\lambda°(OH^-)$, lead respectively to the values of $\Lambda°$ for $Sr(OH)_2$ and $SrCl_2$. The importance of these independent, accurate values of $\Lambda°(SrCl_2)$ and $\Lambda°[Sr(OH)_2]$ is illustrated in Figure 3, which shows the limiting behaviour of the equivalent conductivity of the more-highly associated $Sr(OH)_2$ at 625 K and 20 MPa, relative to $SrCl_2$. Equivalent conductivities at finite concentrations were obtained by fitting the TBBK model to our experimental conductivity data for strontium chloride and strontium hydroxide, Λ^{exp}, reported in Tables 1 and 2, respectively. The fitted values, Λ^{TBBK}, are also tabulated in these tables. The differences between experimental equivalent conductivities and the TBBK fits are included in Tables 1 and 2, and plotted in Figure 4.

3.3   Association Constants

The association constants obtained from the TBBK fits to our data for strontium chloride and strontium hydroxide, are tabulated in Table 5. The first association constants, K_{A1}, were found to be statistically significant over the entire range of temperature and are plotted in Figure 5. Statistically significant formation constants, K_{A2}, for the neutral ion pairs, $SrCl_2^0$ and $Sr(OH)_2^0$, were observed for temperatures $T \geq 445$ K (Figure 6).

The density model of Mesmer et al.[39] (eq 14) was used to represent these association constants over the temperature range investigated. The expression is consistent with the known, very strong dependence of partial molar properties of electrolytes on density associated with the high compressibility of water under near-critical conditions.[1,2.] It takes the form:

$$\log K_{A,m} = a + \frac{b}{T} + \frac{c}{T^2} + \frac{d}{T^3} + \left[e + \frac{f}{T} + \frac{g}{T^2} \right] \cdot \log \rho_w$$

(14)

where the constants a to g are adjustable fitting parameters; ρ_w (kg·m^3) is the density of water at the temperature and pressure of interest, taken from Wagner and Pruss.[24] Many different combinations of fitting parameters were tested. Statistically significant improvement was not obtained when using more than two parameters. The results are tabulated in Table 6 and plotted in Figures 5 and 6.

No combination of parameters yielded a fit to $K_{A,1}$ for strontium chloride with an average relative absolute difference better than 14%. The best results were acquired when using parameters a and e (fit #1), or b and f (fit #2). The latter which was slightly more accurate, is consistent with the form of the "density" model reported by Anderson et al.[40] This model leads to the following simple expressions for the standard partial molar properties, $\Delta H_m°$, $\Delta C_{p,m}°$ and $\Delta V_m°$ which is useful for extrapolating data from 298.15 K.

$$\Delta H_m{}^\circ = -R\ln 10\left[b + f \cdot \log \rho_w\right] - RT \cdot f \cdot \alpha_w \qquad , \qquad (15)$$

$$\Delta C_{p,m}{}^\circ = -f \cdot RT\left(\partial \alpha_w / \partial T\right)_p \qquad\qquad (16)$$

and

$$\Delta V_m{}^\circ = -f \cdot R \cdot \beta_w \qquad . \qquad\qquad (17)$$

Here, α_w and β_w are the thermal expansivity and isothermal compressibility of water at the temperature and pressure of $K_{A,m}$.

For the first association constants of strontium hydroxide, $K_{A,1}[\mathrm{Sr(OH)^+}]$, both combinations of the adjustable parameters yielded relative absolute deviations of better than 4 percent, with the a and e parameters slightly more accurate. Statistically significant results for the second association of strontium hydroxide, $K_{A,2}[\mathrm{Sr(OH)_2{}^0}]$, were obtained only at the five highest experimental temperatures. Values of the a and e, or b and f parameters are also listed in Table 6. The parameter combinations (a and f), and (b and e), yielded the best statistical fit to log K_{A2} for the formation of $\mathrm{SrCl_2{}^0}$. These were also included in Table 6.

4. Comparison with Association Constants from Previous Studies.

4.1 Strontium Chloride Ion Pairs, $\mathrm{SrCl^+}$ and $\mathrm{SrCl_2{}^0}$

The only other temperature-dependant values for the first stepwise association constant for $\mathrm{SrCl^+}$ are the results obtained by Majer and Stulik[41] over the temperature range 288 to 358 K. The values for K_{A1} in Table 5 are higher than those reported in Majer and Stulik's paper, by almost an order of magnitude. However, Majer and Stulik[41] neglected the non-ideality of their solution when they reported their

14

equilibrium constant. We have corrected their results using the Pitzer model adopted by Mendez de Leo and Wood.[35] Details on the ionic strength correction can be found in their paper. Neglecting uncertainties in the correction, this treatment yields the value $K_{A1} = 5.25 \pm 0.08$ at 298.15 K and 0.1 MPa, in reasonable agreement with our result. These corrected values are plotted in Figure 7, along with our results from Table 5.

Figure 7 includes a plot of the association constants for $SrCl^+$ estimated from the Helgeson-Kirkham Flowers-Tanger ("HKF") equation of state, based on parameters regressed by Sverjensky et al.[6] The values for the standard molar Gibbs energy of formation of $SrCl^+$ at 298.15 K in the HKF database were based on the experimental equilibrium quotients from Majer and Stulik.[41] with no correction for the ionic strength of the solutions. The parameters for the standard partial molar entropy and the temperature dependence of $C_p°$ and $V°$, were estimated from correlations based on the data from Majer and Stulik for $SrCl^+$, and literature values for SrF^+ and BaF^+; the chloro complexes of Ca^{2+}, Ag^+, Pb^{2+}, Ba^{2+}; and the neutral species $KHSO_4^0$, $NaHSiO_3^0$ and $AgNO_3^0$. The plot in Figure 7 suggests that the discrepancy with our experimental formation constants is due to the use of uncorrected values from Majer and Stulik to calculate $\Delta_f G°(SrCl^+)$ at 298.15 K.

It is interesting to compare our results for first association constant of $SrCl^+$ at $p = 20$ MPa with those of $CaCl^+$ measured by Mendez de Leo and Wood,[35] at $p = 17.6$ MPa. Their results are included in Figure 7, along with literature values from the literature and the estimated values from the HKF parameters reported by Sverjensky et al.[6] The plot also includes values from the low temperature studies by Johnson and Pytkowicz[42] and Majer and Stulik[41] which have been corrected for ionic strength effects, using the Pitzer treatment reported by Mendez de Leo and Wood.[35] Equilibrium constants reported by Gillespie et al.[43] and Oscarson at al.[44] were derived from experimental measurements of enthalpy of dilution. Mendez de Leo and Wood suggested that Oscarson et al.'s equilibrium constants[44] might be in error because of their choice of an overly simple activity coefficient model, but noted that the resulting values for standard enthalpy of reaction and activity coefficients were in good agreement with the earlier results of Gillespie et al.[43] The inconsistency observed between the experimental

sources and the HKF predictions arises because Sverjensky et al.[6] based the regression of their HKF

parameters on Majer and Stulik's data as published, without applying an activity coefficient

correction.[45]

It is interesting to note that the first stepwise association constant for $CaCl^+$ reported by Mendez de

Leo and Wood,[35] and Gillespie et al.[43] are systematically more positive than those for $SrCl^+$ by 0.1 to

0.3 in log K_{A1} at temperatures above ~375 K. These differences are greater than the combined

experimental uncertainties. Mendez de Leo and Wood[35] derived their association constants from

conductivity data measured with the same apparatus used in the present study, and the data treatment we

have adopted here is also identical to theirs. As a result, we expect differences in the two sets of data to

be largely free of systematic errors. We note that their data point at 473 K is suspicious according to its

high standard error compared to those at other temperatures, reinforcing our observation that the

association constants for $CaCl^+$ and $SrCl^+$ are very similar.

No experimental measurements of the association constants to form the neutral ion pair, $SrCl_2^0$, have

been reported in the literature. There are also no HKF parameters for $SrCl_2^0$ in the paper by Sverjensky

et al.[6] or in other HKF on-line databases.

4.2   Strontium Hydroxide Ion Pairs, $SrOH^+$ and $Sr(OH)_2^0$

No experimental values for the formation constants of $SrOH^+$ and $Sr(OH)_2^0$ at elevated temperatures

have been reported in the literature, however values for the HKF parameters of $SrOH^+$ have been

estimated by Shock et al.[11] These HKF parameters are based on the value log K_{A1} = 5.1 ± 1 at 298.15

K, taken from Baes and Mesmer's critical compilation[10] which was taken from potentiometric

measurements by Carell and Olin.[46] This compares with our value of log K_{A1} = 13.9 ± 5.6 at 295.3 K,

reported in Table 5. Carell and Olin's measurements were made in a supporting electrolyte of 3 mol·L^{-1}

$NaClO_4$, and the difference may be due to the activity coefficient correction used by Baes and Mesmer.

At temperatures above 398 K, the values of log K_{A1} predicted by the HKF parameters of Shock et al.[11]

are larger than our experimental results, by about an order of magnitude. For example, Shock's value of $K_{A1} = (7.328) \cdot 10^4$ at 598.15 K and 20 MPa compares to our values of $K_{A1} = (5.901 \pm 0.855) \cdot 10^3$. We note these values are based on HKF parameters derived from linear correlations between the standard molar entropies of formation, $\Delta_f S^o$, and standard partial molar properties (V^o and C_p^o) of the hydroxy-complexes with the standard molar entropies of formation of the alkaline earth cations. These simple correlations were based on values for the transition metal species MOH^+ from Baes and Mesmer's critically evaluated values of K_{A1} at 298.15 K for nickel, cobalt, iron and lead, and a few less accurate values of ΔS_{A1}^o derived from the temperature dependence of K_{A1}. Although Shock et al.[11] did not report uncertainty limits, the propagated error associated with the high temperature values of K_{A1} must be rather large, at least an order of magnitude. Moreover, the hydroxides in transition metal hydroxide complexes are chemically-bonded ligands, while those in $SrOH^+$ are thought to be contact, solvent-separated, and solvent-solvent-separated ions pairs.[47] As a result, the correlations based on transition metal complexes may not be valid. No HKF parameters were reported for the second strontium hydroxide species, $Sr(OH)_2^0$.

5. Discussion.

5.1 Temperature Dependence of Limiting Conductivities

The classical interpretation of ionic conductivities is summarized in the review paper by Kay.[48] Kay's treatment is based on based on the Frank-Wen model for ionic hydration,[49] in which perturbations caused by the ion on the hydrogen-bonding "structure" of the bulk water that surrounds it are inferred from the temperature dependence of the Walden product ratio,

$$R_{298}^T = \frac{\left(\lambda^\circ \eta_w\right)_T}{\left(\lambda^\circ \eta_w\right)_{T_{Ref}}}, \qquad (18)$$

relative to a reference temperature T_{Ref} = 283.15 K. "Structure-breaking" ions are defined to be those with $R_{283}{}^T$< 1, and "structure-making" ions are those with $R_{283}{}^T$ > 1. In the Frank-Wen model, "structure-breaking" behaviour is associated with large ions having a low surface charge density which are less strongly hydrated, but disrupt the three dimensional hydrogen bonding in the surrounding water. Small ions with high surface charge densities are known to be surrounded by a tightly bound first hydration shell, which is not strongly affect by temperature or pressure, so that $R_{283}{}^T \approx 1$. "Structure-making" behaviour is thought to arise from small polyvalent M^{2+} and M^{3+} ions that orient water molecules in the second hydration shell, and large ions with hydrophobic surfaces, such as the tetra alkyl ammonium ions, that are surrounded by a shell in which water molecules are more strongly hydrogen bonded to one another than is the case in bulk water. A modern interpretation of this classification that includes thermodynamic transfer properties and spectroscopic results is given by Marcus.[50]

The nature of ionic hydration is altered profoundly by dramatic changes in the hydrogen bonded "structure" of liquid water that take place as temperatures rise from 273 K towards the critical point, and densities decrease. For example, the isothermal compressibility of liquid water increases to infinity at the critical temperature and pressure (T_c = 647.10 K, p_c = 22.06 MPa, ρ_c = 322 kg·m^{-3}); the dielectric constant drops from a value of 78.40 at 298.15 K to a value of 13.59 at 625 K and 20 MPa; and the hydrogen bonded coordination number of water drops from ~4 at ambient conditions to ~2.1 at 600 K at p = 20 MPa.[51] The first hydration shell of most ions is relatively unaffected by the changes in temperature and density, however the perturbations in the short-range interactions of the hydrated ion with the surrounding water decrease with increasing temperature, as water becomes less "structured". At temperatures above ~400 K, the dominant effect is the long-range polarization of the bulk solvent due to charge-dipole interactions. As the compressibility of water becomes very large, long-range ion-solvent polarization interactions dominate.[3,39] This is consistent with the effect of the sharp drop in the dielectric constant of water on ion-solvent interactions as described by the classical Born equation.[3] As a

result, the Walden product ratio expressed by eq 18, would be expected to decrease with increasing temperature, due to the viscous drag associated with a more densely packed "hydration" sphere of oriented solvent molecules around each of the ions. This picture is also in agreement with the compressible continuum model for ionic transport in high temperature water by Xiao and Wood,[52] which describes these electrostriction and electroviscosity effects and their influence on the Walden product in high temperature water.

Figure 8 presents plots of the Walden product ratio $R_{298}{}^T$ for the ions Sr^{2+}, Na^+, OH^-, Cl^- and $CF_3SO_3{}^-$, based on the values of $\lambda°$ tabulated in Tables 3 and 4 and a reference temperature $T_{Ref} = 298.15$ K. Based on Kay's interpretation of the values of $R_{283}{}^T$ near ambient conditions and Marcus' classification, Na^+ is considered to be a borderline ion with a strongly-bound first hydration shell. In the Marcus classification, Sr^{2+} and OH^- are classified as "structure-makers" at ambient conditions, with well-defined first hydration spheres, hydrogen-bonded to partially oriented water molecules in the second hydration sphere. The anions Cl^- and $CF_3SO_3{}^-$ are "structure-breakers" with loosely-bound first hydration spheres that provide excess mobility that is more pronounced at temperatures below 298 K and decreases with increasing temperature.

The results in Figure 8 clearly show this decrease. The Walden product ratios, $R_{298}{}^T$, of the cations at 600 K are lower by ~15 percent than those at 298 K, while those of the anions are lower by ~25 percent. The value for OH^- drops by ~ 60 percent. The hydroxide ion is a special case because at 298 K conductivity takes place by both diffusion and proton-hopping, with proton hopping the dominant mechanism.[53-55] At elevated temperatures, proton hopping is much less important, and the diffusion mechanism dominates.[56]

These conclusions from classical models are supported by both experimental studies and computational tools.[50,57,58] Solvent polarization effects are reflected in the standard partial molar volumes of aqueous ions which rise to a maximum at ~ 330 to 360 K as short-range hydration effects become less important, then decrease towards large negative values at the critical point due to the

electrostriction caused by long-range solvent polarization.[3,39,59] These conclusions are also supported by molecular dynamics (MD) simulations of SrCl$_2$ solutions under hydrothermal conditions by Svishchev et al.[60] Pioneering MD studies by Balbuena et al.,[61] showed that the strongly bound first shell of both cations and anions persists well into the high-temperature, low density range of supercritical water, and a well-defined second shell also persists into this region for the divalent cations. A more complete discussion of ionic hydration of Sr^{2+}, Cl$^-$ and OH$^-$ under these conditions is given in the review by Seward and Driesner,[62] and Driesner.[63]

5.2 Strontium Association under Hydrothermal Conditions.

The temperature-dependent first and second association constants for Sr^{2+} plotted in Figures 5 to 7, log K_{1A} and log K_{2A}, can be interpreted using classical models, and modern spectroscopic and simulation results. The classical explanation for temperature dependence of association constants log K_{1A} and log K_{2A}, which favours association at elevated temperatures, has been described by Mesmer et al.[39] and Mesmer et al.'s interpretation is based on the "density" model, eq 14. The $1/T$ terms are thought to be an empirical fit to the short-range hydrogen bonding "structure-making" or "structure-breaking" hydration effects that dominate new ambient condition, while the terms associated with log ρ_w describe the long-range polarization effects associated with the high compressibility of water at elevated temperatures. The association reaction is driven by the change in entropy associated with the formation the large hydration sphere about ions due to the increasingly high compressibility of water at elevated temperatures, and their release into the bulk solvent when a neutral or less highly charged ion pair is formed. An equivalent explanation is given by the HKF model for the chemical potential of aqueous ions[3] and by the Bjerrum or Fuoss models for ion association. In both approaches, the sharp drop in the dielectric constant of water with increasing temperature, noted in Section 5.1, destabilizes highly charged ionic species relative to those with lower charge. The HKF model is applicable to distinct chemical species, such as transition metal hydroxides, while the Bjerrum or Fuoss models describe the

formation of ion pairs. A recent study of $CuSO_4$ (aq) by UV-visible spectroscopyunder hydrothermal conditions, by Mendez de Leo et al.,[64] demonstrated that the Bjerrum model includes the contribution of both solvent-shared-ion-pairs (SShIP) and contact-ion-pairs (CIP), in equilibrium with one another. It is interesting to note that the value of K_{1A} for the formation of $SrOH^+$ is larger than that for $SrCl^+$ by an order of magnitude at all temperatures (Figure 5). The hydroxide and chloride ions are isoelectronic, with nearly identical crystallographic radii,[65] so that the difference must arise from hydrogen-bonding effects. The second stepwise association constant K_{2A} for the hydroxide (Figure 6) is also bigger than that of the chloro species, presumably for the same reason.

Chialvo et al.[66] have compared experimental ion association constants for NaCl from flow conductivity measurements in very high temperature water at low, sub-critical densities with the results obtained by molecular simulations. They noted the presence of two kinds of ion pairs along the 773 K isotherm: a weak solvent-shared ion pair (SShIP) at ~4.3 Åand a stronger contact ion pair (CIP) at ~2.4 Å. They observed that the CIP becomes stronger as the density decreased, as the opposite is the case for the SShIP. The isochoric-temperature derivative changes sign at $\rho_w \approx 40$ kg·m^{-3}, leading to some challenges in modelling such systems. The results show that caution must be exercised in using dielectric-continuum models for treating ion-pair association in aqueous environments at extreme conditions, as noticeable differences were observed when $\rho_w < 400$ kg·m^{-3}. They show that fully electrostatic models, such as those by Bjerrum and Fuoss, cannot account for the inhomogeneity in the distribution of water molecules clustered around the ion in low density supercritical steam, and the fact that the solvent dielectric constant is strikingly modified at proximity of charged species. This is reflected in inability of primitive models to account for SShIP ion pairs and the location and strength of CIP ion pairs.

Molecular dynamics studies on the hydration and association of aqueous alkaline earth chlorides have been carried out by Larentozos and Criscenti[67] at ambient conditions, and by Zhu et al.,[68] under supercritical conditions. While less extensive, the results are similar to those reported by Chialvo et al.

for aqueous NaCl, discussed above. The strength of the ion-water interaction with the first hydration shell is strongest for Mg^{2+} and decreases with increasing ionic radius. As expected, the alkaline earths show little or no ion pairing at 298 K. Both contact and solvent separated ion pairs form under supercritical conditions and, under isothermal supercritical conditions, low densities favour contact ion pairs while higher densities favour solvent separated ion pairs. These simulation results are consistent with the EXAFS studies by Seward et al.[69] on 0.1 and 1.0 $mol \cdot kg^{-1}$ solutions of $SrCl_2$ in water and 3 $mol \cdot kg^{-1}$ HCl from ambient temperatures to 573 K, supported by their own molecular dynamics simulation studies. The EXAFS studies support the conclusions of the simulations, noted above. At the highest temperature and chloride concentration, the EXAFS spectra provide experimental evidence for the $SrCl^+$, $SrCl_2^0$ and $SrCl_3^-$ contact ion pairs. Above 543 K, in 3 $mol \cdot kg^{-1}$, there was also evidence for the presence of clusters with Sr-Sr bonds.

Although they were carried out at much higher concentrations than our conductance measurements (1 $mol \cdot kg^{-1}$ $SrCl_2$ in 3 $mol \cdot kg^{-1}$ Cl^-) vs (0.2 $mol \cdot kg^{-1}$ $SrCl_2$), these EXAFS and simulation results support the conclusion that the ion-pair formation constants for $SrCl^+$ reported in Table 5, represent the equilibrium mixture of CIP and SShIP ion pairs. For $SrCl_2^0$, it seems likely that at least one of the two chlorides has replaced a water of hydration in the first shell with the second water in either the first or second hydration sphere. In the absence of experimental evidence or systematic simulation studies, to speculate on the structure of the hydroxide species $SrOH^+$ and $Sr(OH)_2^0$ would be premature.

6.   The Distribution of Strontium Species in High Temperature Water

The distribution of strontium species in hydrothermal solutions is of considerable interest to the nuclear and petroleum industries who seek to control the production of radium-rich barium and strontium scale on offshore oil production platforms, and the transport of radioactive ^{90}Sr fission products released from fuel failures in nuclear power reactors. This is a particular concern for the proposed Generation IV Supercritical-Water-Cooled (SCWR) reactors which will operate a direct-cycle primary coolant circuit with water at temperatures up to 873 K and 25 MPa.[70] Speciation diagrams were

calculated from the experimental association constants in Table 5 using the values from the TBBK model, and self-consistent activity coefficients.[28]   The results for $Sr(OH)_2$ and $SrCl_2$ at experimental temperatures and pressures, over the full range of concentrations are plotted in Figures 9 and 10, respectively. As is clear from the ion association constant plots in Figures 5 and 6, the formation constants for $Sr(OH)^+$ are stronger than those for $SrCl^+$ by an order of magnitude, while the stepwise equilibrium constants for forming $Sr(OH)_2{}^0$ from $Sr(OH)^+$ are stronger than those of $SrCl_2{}^0$ by about 0.5 orders of magnitude. As a result, the $Sr(OH)_2$ solutions are more strongly ion-paired than $SrCl_2$ at all temperatures.

   The formation constants for the strontium hydroxide species are significant, because they are the first to be reported at such high temperatures. They are particularly important to the nuclear industry, because ^{89}Sr and ^{90}Sr are fission products that can be released into the primary coolant of nuclear reactors from fuel failures. The proposed Generation IV supercritical-water-cooled reactor[70,71] will be based on a direct cycle coolant circuit the carries supercritical water from the reactor core into the turbines a pressure of 25 MPa and temperatures from 570 K to 850 K. Strontium fission products form as the oxide SrO(s) in UO_2 fuel pellets and hydrolyze to $Sr(OH)_2$ when exposed to coolant. Under bulk coolant conditions, the hydroxide concentration will be $\sim 10^{-4}$ mol·kg^{-1}. From the speciation diagram in Figure 9, it appears that the hydroxy complexes will be the dominant strontium species in solution, so that the dissolution reaction can be expressed as

$$Sr(OH)_2(s) \leftrightarrows SrOH^+(aq) + OH^-(aq) \tag{19}$$

   and

$$Sr(OH)_2(s) \leftrightarrows Sr(OH)_2^0(aq) \quad . \tag{20}$$

A full assessment of the risk of fission product carry-over to the turbines will require values for the solubility product of $Sr(OH)_2(s)$ from 523 to 923 K using eqs 19 or 20, along with extrapolated values

for the ion pair formation constants from the data plotted in Figures 5 and 6, and an appropriate chemical equilibrium and transport model for simulating coolant chemistry along the reactor core and into the turbine. The results from this study provide a strong foundation for doing so.

7. Conclusions

This work reports the first conductivity measurements on dilute aqueous solutions of $Sr(OH)_2$ and $SrCl_2$ at solvent densities from 1000 to 600 kg·m^{-3}, and temperatures above 350 K up to temperatures approaching the critical point of water. With the exception of the studies on the alkali metal sulfate/bisulfates by Hnedkovsky et al.[15] and Sharygin et al.[23,72] in this same instrument, these are the first reported ion pair formation constants for an asymmetric 1:2 or 2:1 electrolyte to be measured under these conditions. While its relatively high solubility allows ion pair formation in aqueous strontium chloride to be studied by other, complementary techniques, the equilibrium constants for the formation of $SrOH^+$ and $Sr(OH)_2^0$ could not have been obtained by any other method. As noted above, the stability of $SrOH^+$ and $Sr(OH)_2^0$ was established to be greater than that of the $SrCl^+$ and $SrCl_2^0$ ion pairs, and the availability of accurate association constants for these species is of considerable interest to the modelling of strontium transport in nuclear power stations and hydrothermal geochemical systems.

Sub-critical and supercritical aqueous solutions, in the range 550 to 800 K are of increasing importance in the development of new energy and manufacturing technologies, technologies, and for understanding the formation of ore bodies by vapour transport processes. These solutions are characterized by their small dielectric constants and high solvent compressibilities, that can stabilize unusual species and give rise to physical and chemical processes whose mechanisms are not fully understood. Chialvo et al.[66] have observed that the flow conductivity cell pioneered by R.H. Wood,[12, 15,16,18] used in this work, is one of the most promising tools for studying speciation in low density solutions under these extreme conditions, because it allows measurements to be made at ionic concentrations as low as $2 \cdot 10^{-5}$ mol·kg^{-1}, two orders of magnitude below previous designs. The

measurements reported here illustrate the power of this instrument; indeed, they could not have been made with any other technique.

REFERENCES

1. D. A. Palmer, R. Fernandez-Prini and A. H. Harvey, eds. *Aqueous Systems at Elevated Temperatures and Pressures: Physical Chemistry in Water, Steam and Aqueous Solutions*; Elsevier Academic Press, Amsterdam, 2004.

2. H. Weingärtner and E. U. Franck, *Angew. Chem. Int. Ed.*, 2005, 44, 2672.

3. E. L. Shock, E. H. Oelkers, J.W. Johnson, D. A. Sverjensky and H. C. Helgeson, *J. Chem. Soc. Faraday Trans.,* 1992, 88, 803.

4. J. Sedlbauer, J. P. O'Connell and R. H. Wood *Chem. Geol.*, 2000, 163, 43.

5. A. Anderko and M. M. Lencka, *Ind. Eng. Chem. Res.,* 1997*,* 36, 1932.

6. D. A. Sverjensky, E. L. Shock and H. C. Helgeson, *Geochim. Cosmochim. Acta,* 1997, 61, 1359.

7. E. L. Shock and C. M. Koretsky, *Geochim. Cosmochim. Acta,* 1993, 57, 4899.

8. V. Valyashko, Ed. Hydrothermal Properties of Materials; John Wiley & Sons, Ltd.: New York, 2008.

9. D. J. Wesolowski, L. M. Ziemnak, L. M. Anovitz, M .L. Machesky, P. Benezech and D. A. Palmer, (2004). Solubility and Surface Adsorption Characteristics of Metal Oxides. In D. A. Palmer, R. Fernandez-Prini and A. H. Harvey (Eds.). Aqueous Systems at Elevated Temperatures and Pressures (chap. 14, pp. 493-595). Amsterdam, The Netherlands: Elsevier.

10. C. F. Jr. Baes and R. E. Mesmer, *The Hydrolysis of Cations*. Robert E. Krieger Publishing, F. L. Malibar, 1986, Reprint with corrections of the 1976 edition by Wiley.

11. E. L. Shock, D. C. Sassani, M. Willis and D. A. Sverjensky, *Geochim. Cosmochim. Acta* 1997, 61, 907.

12. G. H. Zimmerman, M. S. Gruskiewicz and R. H. Wood, *J. Phys. Chem.*, 1995, 99, 11612.

13. P. C. Ho, H. Bianchi, D. A. Palmer and R. H. Wood *J. Solution Chem.,* 2000, 29, 217-235.

14. A. V. Sharygin, R. H. Wood, G. H. Zimmerman and V. N. Balashov, *J. Phys. Chem. B,* 2002, 106, 7121.

15. L. Hnedkovsky, R. H. Wood and V. N. Balashov, *J. Phys. Chem. B,* 2005, 109, 9034.

16. G. H. Zimmerman, H. Arcis and P. R. Tremaine, *J. Chem. Eng. Data,* 2012, 57, 3180.

17. J. A. Rard and D. G. Miller, *J. Chem. Eng. Data,* 1982, 27, 342.

18. G. H. Zimmerman, H. Arcis and P. R. Tremaine, *J. Chem. Eng. Data,* 2012, 57, 2415.

19. A. J. Bard and L. R. Faulkner, Electrochemical methods: Fundamentals and applications, John Wiley & Sons, New York, New York, 2001.

20. V. N. Balashov, M. V. Fedkin and S. N. Lvov, *J. Electrochem. Soc.,* 2009, 156, C209.

21. *Impedance Spectroscopy, Theory, Experiment and Applications*, Editors E. Barsoukov and J. R. MacDonald, Wiley-Interscience, 2005.

22. G. H. Zimmerman and H. Arcis, *J. Solution Chem.* (accepted)

23. A. V. Sharygin, I. Mokbel, C. Xiao and R. H. Wood, *J. Phys. Chem. B,* 2001, 105, 229.

24. W. Wagner and A. Pruss, *J. Phys. Chem. Ref. Data,* 2002, 31, 387.

25. P. R. Tremaine, K. Zhang, P. Benezech and C. Xiao, (2004). Ionization Equilibria of Acids and Bases under Hydrothermal Conditions. In D. A. Palmer, R. Fernandez-Prini, A. H. Harvey (Eds.). Aqueous Systems at Elevated Temperatures and Pressures (chap. 13, pp. 441-492). Amsterdam, The Netherlands: Elsevier.

26. E. L. Shock, and H. C. Helgeson, *Geochim. Cosmochim. Acta,* 1988, 52, 2009.

27. H. C. Helgeson, *Appl. Geochem.,* 1992, 7, 291.

28. P. Turq, L. Blum, O. Bernard and W. Kunz, *J. Phys. Chem.,* 1995, 99, 822.

29. H. Bianchi, I. Dujovne and R. Fernández-Prini, *J. Solution Chem.,* 2000, 29, 237.

30. L. Blum and S. Hoye, *J. Phys. Chem.,* 1977, 81, 1311.

31. D. P. Fernandez, A. R. H. Goodwin, E. W. Lemmon, J. M. H. Levelt-Sengers and R. C. Williams, *J. Phys. Chem. Ref. Data,* 1997, 26, 1125.

32. M. L. Huber, R. A. Perkins, A. Laesecke, D. G. Friend, J. V. Sengers, M. J. Assael, I. N. Metaxa, E. Vogel, R. Mares and K. Miyagawa, *J. Phys. Chem. Ref. Data,* 2009, 38, 101.

33. A. V. Bandura and S. N. Lvov, *J. Phys. Chem. Ref. Data,* 2006, 35, 15.

34. Y. Marcus, *Ion Solvation*; Wiley: New York, 1985.

35. L.P. Méndez De Leo and R. H. Wood, *J. Phys. Chem. B,* 2005, 109, 14243.

36. W.M. Marshall, *J. Chem. Phys*., 1987, 87, 3639.

37. P. C. Ho, D. A. Palmer and R. H. Wood, *J. Phys. Chem. B,* 2000, 104, 12084.

38. H. Bianchi, H. R. Corti and R. Fernandez-Prini, *J. Solution Chem.,* 1988, 17, 1059.

39. R.E. Mesmer, W.L. Marshall, D.A. Palmer, J. M. Simonson and H.F. Holmes, *J. Solution Chem.,* 1988, 17, 699.

40. G. M. Anderson, S. Castet, J. Schott and R.E. Mesmer, *Geochim. Cosmochim. Acta,* 1991, 55, 1769.

41. V. Majer and K. Stulik, *Talanta,* 1982, 29, 145.

42. K. S. Johnson and R. M. Pytkowicz, *Am. J. Sci.,* 1978, 278, 1428.

43. S. E. Gillespie, J. L. Oscarson, X. Chen and C. Pando, *J. Solution Chem.,* 1992, 21, 761.

44. J. L. Oscarson, S. E. Gillespie, X. Chen, P. C. Schuck and R.M. Izatt, *J. Solution Chem.,* 2001, 30, 31.

45. D. A. Sverjensky, Private Communication.

46. B. Carell and A. Olin *Acta Chem. Scand.,* 1961, 15, 727.

47. G. Hefter, *Pure Appl. Chem*., 2006, 78, 1571.

48. R. L. Kay, *Pure & Appl. Chem*., 1991, 63, 1393.

49. H. S. Frank and W. Y. Wen, *Discuss. Faraday Soc.,* 1957, 24, 133.

50. Y. Marcus, *J. Phys. Chem. B,* 2009, 113, 10285.

51. M. Nakahara, Structure, Dynamics, and reactions of Supercritical Water Studied by NMR and Computer Simulation. Water, Steam, and Aqueous Solutions for Electric Power. Advances in Science and technology. Proceedings of the 14th International Conference on the Properties of Water and Steam in Kyoto. Aug 29-Sep 3, 2004.

52. C. Xiao and R. H. Wood, *J. Phys. Chem. B,* 2000, 104, 918.

53. Y. Tada, M. Ueno, N. Tsuchihashi and K. Shimizu, *J. Solution Chem*., 1992, 21, 971.

54. Y. Tada, M. Ueno, N. Tsuchihashi and K. Shimizu, *J. Solution Chem*., 1993, 22, 1135.

55. Y. Tada, M. Ueno, N. Tsuchihashi and K. Shimizu, *J. Solution Chem*., 1994, 23, 973.

56. H. Arcis, J. Plumridge and P. R. Tremaine, (to be published).

57. P. G. Kusalik and I. M. Svishchev, *Science,* 1994, 265 (5176), 1219.

58. M. Boero, K. Terakura, T. Ikeshoji, C. C. Liew and M. Parrinello, *J. Chem. Phys*. 2001, 115, 2219.

59. P. R. Tremaine and H. Arcis, *Reviews in Mineralogy & Geochemistry,* 2013, 76, 249.

60. I. M. Svishchev, A. Y. Zasetsky and I. G. Nahtigal, *J. Phys. Chem. C,* 2005, 112, 20181.

61. P. B. Balbuena, K. P. Johnston and P. J. Rossky, *J. Phys. Chem.,* 1996, 100, 2706.

62. T. M. Seward and T. Driesner, (2004). Hydrothermal solution structure: experiments and computer simulations. In D.A. Palmer, R. Fernandez-Prini, A.H. Harvey (Eds.). Aqueous Systems at Elevated Temperatures and Pressures (chap. 5, pp.149-182). Amsterdam, The Netherlands: Elsevier.

63. T. Driesner, *Rev. Mineralogy and Geochemistry,* 2013, 76, 5.

64. L. P. Méndez De Leo, H. L.; Bianchi and R. Fernández-Prini, *J. Chem. Thermodyn.,* 2005, 37, 499.

65. Y. Marcus, *Chem. Rev.*, 2009, 109, 1346.

66. A. A. Chialvo, M. S. Gruszkiewicz and D. R. Cole, *J. Chem. Eng. Data,* 2010, 55,1828.

67. J. P. Larentzos and L. J. Criscenti, *J. Phys. Chem. B,* 2008, 112, 14243.

68. Y. Zhu, X. Lu, H. Ding and Y. Wang, *Molecular Simulations,* 2003, 29, 767.

69. T. M. Seward, C. M. B. Henderson, J. M. Charnock and T. Driesner, *Geochim. Cosmochim. Acta,* 1999, 63, 2409.

70. D. Guzonas, F. Brosseau, P. Tremaine, J. Meesungnoen and J.-P. Jay-Gerin, *Nuclear Technol.*, 2012, 179, 205.

71. D. F. Torgerson, B. A. Shalaby and S. Pang, *Nucl.Eng. Design,* 2006, 236(14-16), 1565.

72. A. V. Sharygin, B. K. Grafton, C. Xiao R. H. Wood and V. N. Balashov, *Geochim. Cosmochim. Acta,* 2006, 70, 5169.

SYNOPSIS TOC.
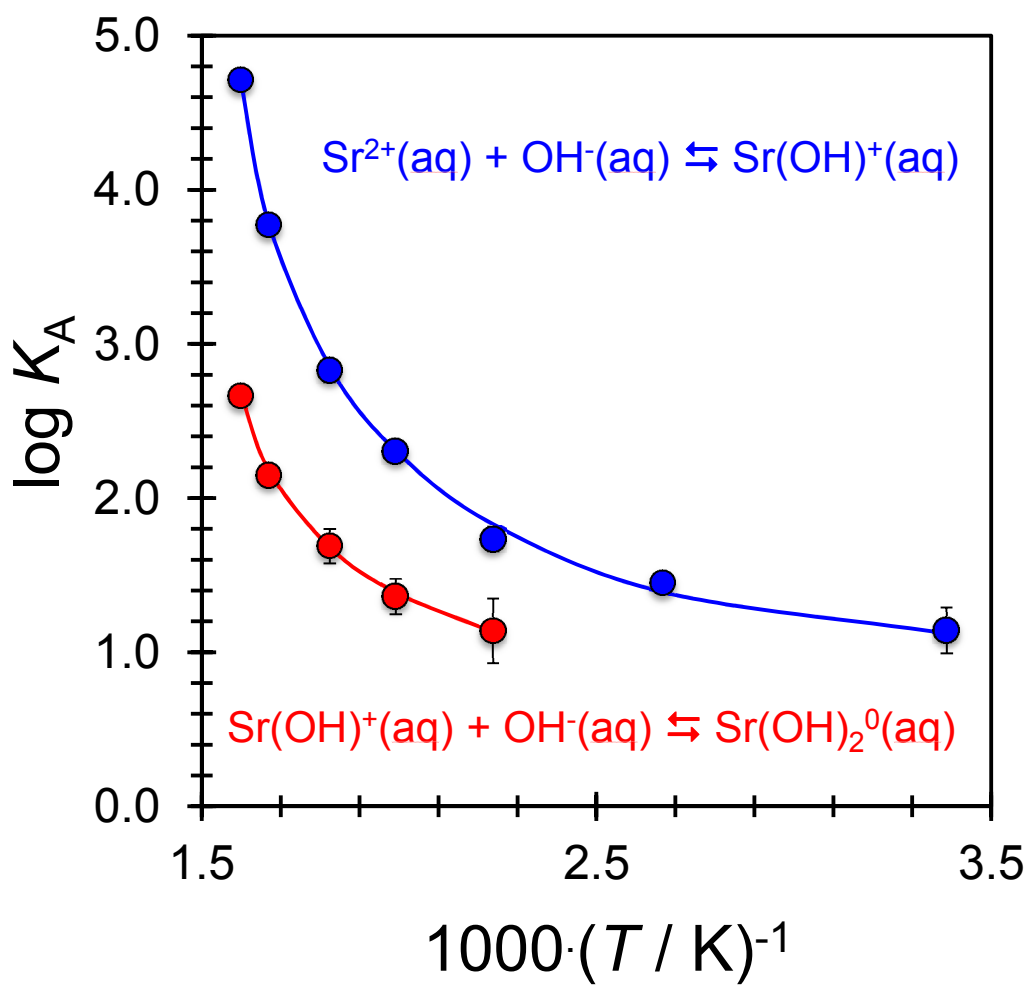
Table 1. Molality, Molarity, Conductivity, Experimental, and Calculated (from the TBBK Equation)

Equivalent Conductivities of Aqueous $Sr(OH)_2$ from 295 K to 625 K at p= 20 MPa.

$10^3 \cdot m$ / $mol \cdot kg^{-1}$	$10^3 \cdot c$ / $mol \cdot L^{-1}$	$\kappa_{soln}^{exp} \cdot 10^6$ / $S \cdot cm^{-1}$	Λ^{exp} / $S \cdot cm^2 \cdot eq^{-1}$			Λ^{TBBK}	$100 \cdot (\Lambda^{exp} - \Lambda^{TBBK}) / \Lambda^{exp}$
T = 295.27 K, p = 17.64 MPa, ρ_w = 1005.6 kg·m^{-3}							
κ_w^{exp}= 1.317·10^{-7} / S·cm^{-1}, κ_w^{th} = 0.5070·10^{-7} / S·cm^{-1}							
0	0	-	-			242.7	-
0.6204	0.6238	289.8	232.2	±	1.0	233.3	-0.47
1.856	1.866	829.5	222.2	±	1.0	226.2	-1.82
3.869	3.891	1699.1	218.3	±	1.0	218.9	-0.28
5.901	5.934	2543.1	214.3	±	1.0	213.6	0.30
7.923	7.968	3365.0	211.1	±	1.0	209.4	0.80
T = 374.84 K, p = 20.87 MPa, ρ_w = 966.64 kg·m^{-3}							
κ_w^{exp}= 12.94·10^{-7} / S·cm^{-1}, κ_w^{th} = 9.271·10^{-7} / S·cm^{-1}							
0	0	-	-			642.2	-
0.4481	0.4332	530.4	610.7	±	2.7	614.0	-0.55
0.4481	0.4332	532.3	612.9	±	2.7	614.0	-0.18
0.5339	0.5161	628.1	607.3	±	2.5	611.4	-0.68
0.5339	0.5161	637.3	616.2	±	2.5	611.4	0.79
2.120	2.049	2367	577.3	±	2.7	577.8	-0.08
4.504	4.354	4777	548.4	±	2.7	548.5	-0.02
6.946	6.715	7072	526.4	±	2.6	528.2	-0.33
8.710	8.421	8716	517.5	±	2.5	516.7	0.14
8.710	8.421	8715	517.4	±	2.5	516.7	0.12
T = 446.79 K, p = 20.95 MPa, ρ_w = 906.05 kg·m^{-3}							
κ_w^{exp}= 34.82·10^{-7} / S·cm^{-1}, κ_w^{th} = 27.71·10^{-7} / S·cm^{-1}							
0	0	-	-			931.2	-
0.534	0.484	855.2	880.4	±	3.9	867.6	1.45
1.934	1.752	2842	810.0	±	3.6	804.8	0.64
4.664	4.226	6208	734.0	±	3.4	735.8	-0.24
6.480	5.872	8239	701.2	±	3.3	704.8	-0.51
8.558	7.756	10438	672.6	±	3.2	676.8	-0.61
13.87	12.57	15729	625.5	±	3.2	625.1	0.07
20.44	18.53	21526	580.7	±	3.2	581.8	-0.19
31.37	28.44	30518	536.4	±	3.3	533.4	0.57

Table 1. (Continued).

$10^3 \cdot m$ / mol·kg^{-1}	$10^3 \cdot c$ / mol·L^{-1}	$\kappa_{soln}^{exp} \cdot 10^6$ / S·cm^{-1}	Λ^{exp} / S·cm^2·eq^{-1}		Λ^{TBBK}	$100 \cdot (\Lambda^{exp} - \Lambda^{TBBK}) / \Lambda^{exp}$
$T = 502.17$ K, $p = 20.86$ MPa, $\rho_w = 844.53$ kg·m^{-3}						
$\kappa_w^{exp} = 47.25 \cdot 10^{-7}$ / S·cm^{-1}, $\kappa_w^{th} = 37.76 \cdot 10^{-7}$ / S·cm^{-1}						
0	0	-	-		1142.5	-
0.2519	0.2128	455.1	1058.4	± 4.7	1047.0	1.08
0.5923	0.5002	1000	995.2	± 4.4	991.1	0.41
1.150	0.972	1805	926.2	± 4.1	926.5	-0.03
3.030	2.559	4106	801.3	± 3.6	804.8	-0.44
5.103	4.311	6284	728.3	± 3.4	731.2	-0.39
10.08	8.52	10676	626.4	± 3.1	633.0	-1.07
20.44	17.28	18567	537.2	± 2.9	534.8	0.44
31.37	26.52	25553	481.8	± 3.0	479.2	0.52
$T = 548.09$ K, $p = 20.57$ MPa, $\rho_w = 779.52$ kg·m^{-3}						
$\kappa_w^{exp} = 48.74 \cdot 10^{-7}$ / S·cm^{-1}, $\kappa_w^{th} = 36.19 \cdot 10^{-7}$ / S·cm^{-1}						
0	0	-	-		1267.0	-
0.1170	0.0912	216.3	1159.1	± 5.4	1130.4	2.47
0.4470	0.3484	697.4	993.7	± 4.4	996.5	-0.28
1.2164	0.9483	1581	831.0	± 3.7	845.3	-1.73
3.709	2.892	3820	659.5	± 3.0	664.5	-0.76
6.547	5.106	5924	579.7	± 2.7	577.4	0.40
10.08	7.86	8175	519.4	± 2.5	515.4	0.78
20.44	15.95	13316	417.3	± 2.2	423.0	-1.36
30.20	23.57	17950	380.7	± 2.3	377.2	0.92

Table 1. (Continued).

$10^3 \cdot m$	$10^3 \cdot c$	$\kappa_{soln}^{exp} \cdot 10^6$	Λ^{exp}		Λ^{TBBK}	$100 \cdot (\Lambda^{exp} - \Lambda^{TBBK}) / \Lambda^{exp}$
/ mol·kg⁻¹	/ mol·L⁻¹	/ S·cm⁻¹			/ S·cm²·eq⁻¹	

T = 598.71 K, p = 20.66 MPa, ρ_w = 680.20 kg·m⁻³
κ_w^{exp} = 55.84·10⁻⁷ / S·cm⁻¹, κ_w^{th} = 23.56·10⁻⁷ / S·cm⁻¹

$10^3 \cdot m$	$10^3 \cdot c$	$\kappa_{soln}^{exp} \cdot 10^6$	Λ^{exp}		Λ^{TBBK}	$100 \cdot (\Lambda^{exp} - \Lambda^{TBBK}) / \Lambda^{exp}$
0	0	-	-		1397.4	-
0.03298	0.02243	55.89	1121.1	± 8.3	1126.5	-0.48
0.06798	0.04624	101.7	1039.5	± 5.7	1039.0	0.05
0.1331	0.0906	170.7	911.5	± 4.4	932.0	-2.25
0.4350	0.2959	431.8	720.1	± 3.2	736.4	-2.26
1.815	1.235	1328	535.4	± 2.4	540.2	-0.89
3.934	2.678	2430	452.6	± 2.1	449.7	0.65
6.547	4.457	3581	401.1	± 1.9	394.1	1.73
10.08	6.866	4732	344.2	± 1.7	349.7	-1.58

T = 625.46 K, p = 20.42 MPa, ρ_w = 593.36 kg·m⁻³
κ_w^{exp} = 40.86·10⁻⁷ / S·cm⁻¹, κ_w^{th} = 12.66·10⁻⁷ / S·cm⁻¹

$10^3 \cdot m$	$10^3 \cdot c$	$\kappa_{soln}^{exp} \cdot 10^6$	Λ^{exp}		Λ^{TBBK}	$100 \cdot (\Lambda^{exp} - \Lambda^{TBBK}) / \Lambda^{exp}$
0	0	-	-		1492.1	-
0.02986	0.01772	32.39	798.7	± 7.1	843.3	-5.58
0.05134	0.03047	49.47	744.8	± 4.8	766.7	-2.94
0.05134	0.03047	49.89	751.7	± 4.9	766.7	-1.99
0.08187	0.04858	71.68	695.6	± 3.8	706.4	-1.55
0.14686	0.08715	114.5	633.8	± 3.1	639.9	-0.97
0.4713	0.2797	294.4	518.9	± 2.3	526.1	-1.37
0.9533	0.5659	524.0	459.4	± 2.0	458.9	0.10
3.934	2.337	1504	320.9	± 1.5	320.8	0.03

Table 2. Molality, Molarity, Conductivity, Experimental, and Calculated (from the TBBK Equation) Equivalent Conductivities of Aqueous $SrCl_2$ from 295 K to 625 K at p= 20 MPa.

$10^3 \cdot m$ / mol·kg^{-1}	$10^3 \cdot c$ / mol·L^{-1}	$\kappa_{soln}{}^{exp} \cdot 10^6$ / S·cm^{-1}	Λ^{exp} / S·cm^2·eq^{-1}			Λ^{TBBK}	$100 \cdot (\Lambda^{exp} - \Lambda^{TBBK}) / \Lambda^{exp}$

T = 295.51 K, p = 17.93 MPa, ρ_w = 1005.6 kg·m^{-3}
$\kappa_w{}^{exp}$= 1.531·10^{-7} / S·cm^{-1}, $\kappa_w{}^{th}$ = 0.5146·10^{-7} / S·cm^{-1}

$10^3 \cdot m$	$10^3 \cdot c$	$\kappa_{soln}{}^{exp} \cdot 10^6$	Λ^{exp}			Λ^{TBBK}	$100 \cdot (\Lambda^{exp} - \Lambda^{TBBK}) / \Lambda^{exp}$
0	0	-	-			130.1	-
0.5079	0.5108	127.7	124.8	±	0.5	124.9	-0.04
1.156	1.163	284.6	122.3	±	0.5	122.4	-0.07
2.887	2.903	687.8	118.4	±	0.5	118.4	0.06
4.734	4.761	1101	115.6	±	0.5	115.5	0.04
6.834	6.871	1554	113.0	±	0.5	113.1	-0.07

T = 375.72 K, p = 21.06 MPa, ρ_w = 966.11 kg·m^{-3}
$\kappa_w{}^{exp}$= 11.22·10^{-7} / S·cm^{-1}, $\kappa_w{}^{th}$ = 9.498·10^{-7} / S·cm^{-1}

$10^3 \cdot m$	$10^3 \cdot c$	$\kappa_{soln}{}^{exp} \cdot 10^6$	Λ^{exp}			Λ^{TBBK}	$100 \cdot (\Lambda^{exp} - \Lambda^{TBBK}) / \Lambda^{exp}$
0	0	-	-			400.0	-
0.5542	0.5354	407.5	379.5	±	1.7	379.8	-0.09
1.363	1.317	969.3	367.6	±	1.6	368.8	-0.31
3.981	3.846	2685	349.0	±	1.6	348.9	0.03
6.849	6.617	4439	335.4	±	1.6	335.6	-0.06
10.47	10.12	6551	323.7	±	1.6	323.7	0.01

T = 446.10 K, p = 20.92 MPa, ρ_w = 906.70 kg·m^{-3}
$\kappa_w{}^{exp}$= 30.47·10^{-7} / S·cm^{-1}, $\kappa_w{}^{th}$ = 27.53·10^{-7} / S·cm^{-1}

$10^3 \cdot m$	$10^3 \cdot c$	$\kappa_{soln}{}^{exp} \cdot 10^6$	Λ^{exp}			Λ^{TBBK}	$100 \cdot (\Lambda^{exp} - \Lambda^{TBBK}) / \Lambda^{exp}$
0	0	-	-			673.3	-
1.377	1.248	1511	604.0	±	2.7	607.5	-0.59
1.658	1.503	1802	598.2	±	2.7	601.3	-0.51
2.856	2.590	3000	578.7	±	2.6	580.1	-0.25
4.383	3.974	4452	559.8	±	2.6	560.4	-0.11
6.085	5.517	6001	543.6	±	2.5	543.6	0.00
7.827	7.097	7519	529.5	±	2.5	529.8	-0.05
24.23	21.97	20335	462.8	±	2.6	461.3	0.32
61.52	55.78	45121	404.5	±	3.3	402.7	0.44
120.3	109.0	79157	363.0	±	4.4	362.3	0.18
150.9	136.8	95263	348.3	±	5.0	349.1	-0.23
271.8	246.2	153295	311.3	±	7.1	315.7	-1.40
196.1	177.7	118184	332.6	±	5.8	334.6	-0.60

Table 2. (Continued)

$10^3 \cdot m$	$10^3 \cdot c$	$\kappa_{soln}^{exp} \cdot 10^6$	Λ^{exp}			Λ^{TBBK}	$100 \cdot (\Lambda^{exp} - \Lambda^{TBBK}) / \Lambda^{exp}$
/ mol·kg^{-1}	/ mol·L^{-1}	/ S·cm^{-1}	/ S·cm^2·eq^{-1}				

$T = 501.10$ K, $p = 20.96$ MPa, $\rho_w = 844.89$ kg·m^{-3}
$\kappa_w^{exp} = 49.58 \cdot 10^{-7}$ / S·cm^{-1}, $\kappa_w^{th} = 37.78 \cdot 10^{-7}$ / S·cm^{-1}

$10^3 \cdot m$	$10^3 \cdot c$	$\kappa_{soln}^{exp} \cdot 10^6$	Λ^{exp}			Λ^{TBBK}	$100 \cdot (\Lambda^{exp} - \Lambda^{TBBK}) / \Lambda^{exp}$
0	0	-	-			876.5	-
0.2104	0.1778	296.4	819.9	±	3.7	836.4	-2.01
0.8800	0.7435	1170	783.7	±	3.5	790.0	-0.80
1.518	1.283	1951	758.7	±	3.4	762.3	-0.48
5.047	4.265	5786	677.7	±	3.1	680.0	-0.34
10.80	9.13	11185	612.5	±	3.0	616.4	-0.65
15.09	12.76	15084	591.1	±	3.1	587.2	0.66
20.24	17.11	19356	565.6	±	3.1	561.5	0.72
62.48	52.86	49675	469.8	±	3.9	467.7	0.44
123.4	104.5	86649	414.5	±	5.3	418.2	-0.91
195.6	165.8	126528	381.5	±	6.9	388.2	-1.78

$T = 548.54$ K, $p = 20.62$ MPa, $\rho_w = 778.87$ kg·m^{-3}
$\kappa_w^{exp} = 43.24 \cdot 10^{-7}$ / S·cm^{-1}, $\kappa_w^{th} = 36.15 \cdot 10^{-7}$ / S·cm^{-1}

$10^3 \cdot m$	$10^3 \cdot c$	$\kappa_{soln}^{exp} \cdot 10^6$	Λ^{exp}			Λ^{TBBK}	$100 \cdot (\Lambda^{exp} - \Lambda^{TBBK}) / \Lambda^{exp}$
0	0	-	-			1004.0	-
0.1153	0.0898	177.5	964.7	±	4.5	965.7	-0.10
0.4451	0.3467	648.2	928.4	±	4.1	922.5	0.64
0.9890	0.7704	1363	882.1	±	3.9	879.3	0.31
4.088	3.186	4824	756.5	±	3.4	760.3	-0.50
10.07	7.85	10301	655.6	±	3.2	660.9	-0.81
23.89	18.64	20907	560.7	±	3.2	561.2	-0.11
47.23	36.89	36419	493.5	±	3.6	488.6	0.99
101.4	79.4	67604	425.5	±	4.7	420.9	1.07
149.7	117.5	92512	393.7	±	5.7	393.4	0.06
238.3	187.9	115173	374.1	±	6.6	378.9	-1.30
195.6	153.9	135036	359.3	±	7.4	366.8	-2.09

Table 2. (Continued)

$10^3 \cdot m$	$10^3 \cdot c$	$\kappa_{soln}^{exp} \cdot 10^6$	Λ^{exp}			Λ^{TBBK}	$100 \cdot (\Lambda^{exp} - \Lambda^{TBBK}) / \Lambda^{exp}$
/ mol·kg^{-1}	/ mol·L^{-1}	/ S·cm^{-1}				/ S·cm^2·eq^{-1}	

$T = 600.02$ K, $p = 20.65$ MPa, $\rho_w = 676.87$ kg·m^{-3}
$\kappa_w^{exp} = 43.24 \cdot 10^{-7}$ / S·cm^{-1}, $\kappa_w^{th} = 23.10 \cdot 10^{-7}$ / S·cm^{-1}

$10^3 \cdot m$	$10^3 \cdot c$	$\kappa_{soln}^{exp} \cdot 10^6$	Λ^{exp}			Λ^{TBBK}	$100 \cdot (\Lambda^{exp} - \Lambda^{TBBK}) / \Lambda^{exp}$
0	0	-	-			1144.8	-
0.08338	0.05644	126.3	1083.9	±	5.2	1084.0	-0.01
0.2022	0.1369	292.0	1051.9	±	4.7	1038.4	1.29
0.5762	0.3901	748.0	953.6	±	4.2	951.0	0.28
1.051	0.712	1252	876.9	±	3.9	882.6	-0.65
5.051	3.423	4470	652.3	±	3.0	663.1	-1.65
12.67	8.60	9166	532.5	±	2.6	534.9	-0.44
20.49	13.92	13551	486.5	±	2.6	476.0	2.15
20.49	13.92	13221	474.6	±	2.6	476.0	-0.29
44.58	30.41	24460	402.1	±	2.7	398.7	0.85
94.94	65.26	44920	344.1	±	3.4	351.9	-2.26

$T = 625.10$ K, $p = 20.53$ MPa, $\rho_w = 595.51$ kg·m^{-3}
$\kappa_w^{exp} = 14.18 \cdot 10^{-7}$ / S·cm^{-1}, $\kappa_w^{th} = 12.93 \cdot 10^{-7}$ / S·cm^{-1}

$10^3 \cdot m$	$10^3 \cdot c$	$\kappa_{soln}^{exp} \cdot 10^6$	Λ^{exp}			Λ^{TBBK}	$100 \cdot (\Lambda^{exp} - \Lambda^{TBBK}) / \Lambda^{exp}$
0	0	-	-			1254.8	-
0.07865	0.04684	103.7	1091.4	±	4.9	1086.3	0.47
0.1754	0.1045	210.3	999.6	±	4.4	987.0	1.26
0.4153	0.2474	425.6	857.1	±	3.8	857.8	-0.09
0.7569	0.4511	686.6	759.5	±	3.3	763.7	-0.55
1.916	1.143	1400	612.0	±	2.7	626.2	-2.32
3.934	2.349	2462	523.8	±	2.4	532.7	-1.70
7.238	4.329	4064	469.2	±	2.2	463.3	1.26
11.54	6.915	6037	436.4	±	2.1	416.2	4.62
38.11	23.09	15419	333.9	±	2.1	321.6	3.68
38.11	23.09	14927	323.2	±	2.0	321.6	0.50
94.94	58.91	30560	259.4	±	2.5	287.7	-10.94

Table 3 Equivalent Limiting Conductivities and Auxiliary Parameters used for fitting the Sr(OH)$_2$ Data

with the TBBK Equation

T / K	p / MPa	ρ_w / kg·m^{-3}	pK_w	$\lambda°(Sr^{2+})$	$\lambda°(OH^-)$	$\lambda°(H^+)$	$\lambda°(Sr(OH)^+)$
						/ S·cm^2·eq^{-1}	
295.27	17.64	1005.58	14.030	55.6	186.4	335.1	27.8
374.84	20.87	966.64	12.153	202.0	440.1	637.8	100.6
446.79	20.95	906.05	11.364	326.4	604.9	789.8	162.1
502.17	20.86	844.53	11.108	435.5	707.0	855.9	215.7
548.09	20.57	779.52	11.096	496.3	770.6	884.2	245.5
598.71	20.66	680.20	11.351	579.1	818.4	906.2	285.4
625.46	20.42	593.36	11.766	651.5	840.6	912.8	319.7

Table 4 Equivalent Limiting Conductivities and Auxiliary Parameters used for fitting the $SrCl_2$ Data

with the TBBK Equation

T / K	p / MPa	ρ_w / kg·m^{-3}	pK_w	$\lambda°(Sr^{2+})$	$\lambda°(Cl^-)$	$\lambda°(H^+)$	$\lambda°(OH^-)$	$\lambda°(SrCl^+)$
						/ S·cm^2·eq^{-1}		
295.51	17.93	1005.64	14.020	59.1	70.9	336.3	185.0	28.9
375.72	21.06	966.11	14.020	190.2	209.8	640.1	442.4	92.3
446.10	20.92	906.70	11.369	325.0	348.4	788.8	603.6	157.3
501.96	20.96	844.89	11.108	435.1	441.4	855.7	706.6	209.5
548.54	20.62	778.87	11.096	497.1	506.9	884.4	771.1	239.5
600.02	20.65	676.87	11.364	582.0	562.8	906.6	819.4	278.7
625.10	20.53	595.51	11.753	650.2	604.6	912.7	840.2	309.8

Table 5. Experimental Association Constants for Aqueous Strontium Hydroxide and Strontium Chloride

Determined when Fitting the Data with the TBBK Equation

T / K	p / MPa	ρ_w / kg·m^{-3}	pK_w	$K_{A1,m}$			$K_{A2,m}$		
				Sr(OH)$_2$(aq)					
295.27	17.64	1005.58	14.030	13.9	±	5.6	-		
374.84	20.87	966.64	12.153	28.2	±	3.4	-		
446.79	20.95	906.05	11.364	54	±	10	13.8	±	8.6
502.17	20.86	844.53	11.108	200	±	24	23.0	±	6.9
548.09	20.57	779.52	11.096	674	±	119	49	±	14
598.71	20.66	680.2	11.351	5901	±	855	141	±	20
625.46	20.42	593.36	11.766	51844	±	2349	461	±	18
				SrCl$_2$(aq)					
295.51	17.93	1005.64	14.020	2.73	±	0.71	-		
375.72	21.06	966.11	12.139	7.73	±	1.68	-		
446.1	20.92	906.7	11.369	20.4	±	1.0	2.7	±	0.8
501.96	20.96	844.89	11.108	44.4	±	4.1	6.5	±	2.7
548.54	20.62	778.87	11.096	63	±	12	31	±	11
600.02	20.65	676.87	11.364	269	±	51	66	±	21
625.1	20.53	595.51	11.753	1676	±	279	64	±	17

Table 6. Fitted Parameters for the Temperature and Density Dependence of Association Constants, K_A, According to the Density Model, eq 14.

Species	fit #	$a \cdot 10^0$			$b \cdot 10^{-3}$			$e \cdot 10^0$			$f \cdot 10^{-3}$			$\Delta K/K \cdot 100$
$Sr(OH)^+$	1	48.11	±	1.16				-15.65	±	0.41				1.87
$Sr(OH)^+$	2				34.74	±	0.88				-11.46	±	0.31	3.56
$Sr(OH)_2^0$	1	26.03	±	0.91				-8.42	±	0.33				1.03
$Sr(OH)_2^0$	2				19.25	±	0.38				-6.34	±	0.14	0.96
$SrCl^+$	1	31.80	±	5.80	-			-10.32	±	1.98				17.50
$SrCl^+$	2				23.54	±	2.89				-7.766	±	0.982	14.36
$SrCl_2^0$	1	4.886	±	1.250							-0.6722	±	0.2325	8.06
$SrCl_2^0$	2				-2.923	±	0.802	2.41	±	0.61				9.50

* Here $\Delta K/K$ corresponds to $\sum_i^n \frac{1}{n} \cdot \frac{\left| K_{A,i}^{exp} - K_{A,i}^{fit} \right|}{K_{A,i}^{exp}}$, and n is the total number of experimental data points.

FIGURES:
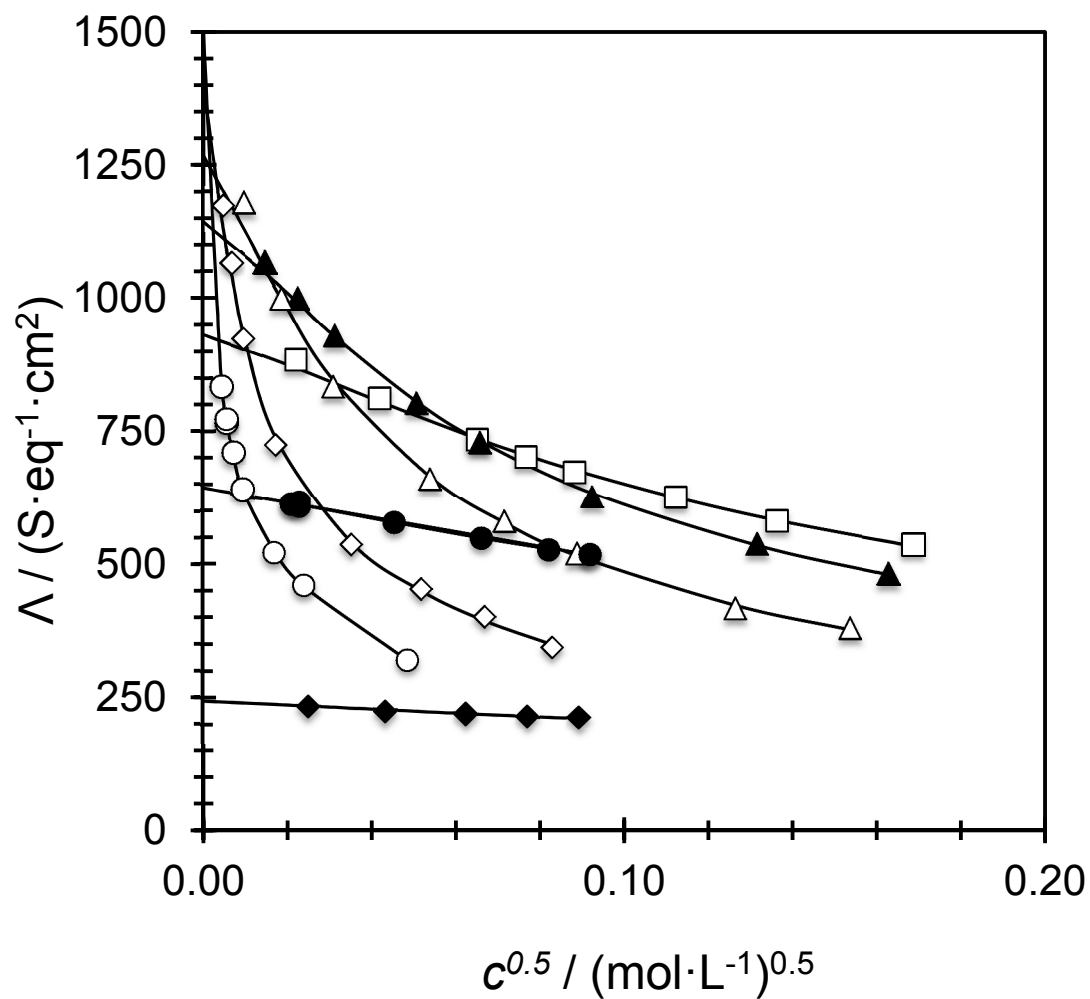
Figure 1. Experimental equivalent conductivity of aqueous $Sr(OH)_2$ from 295 K to 625 K at p = 20 MPa: ◆, 295 K; ●, 375 K.; □, 447 K; ▲, 502 K; △, 548 K; ◇, 599 K; ○, 625 K; plain line, TBBK fit.
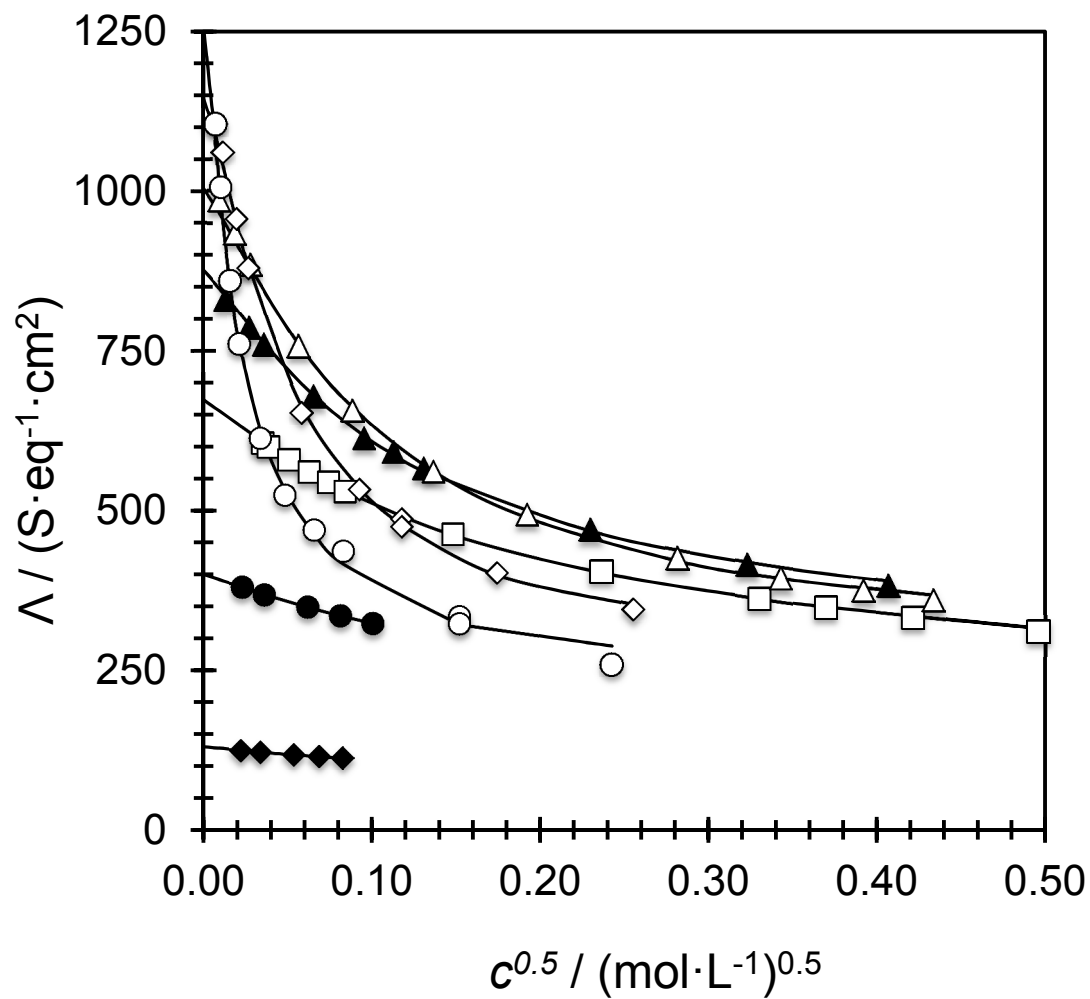
Figure 2. Experimental equivalent conductivity of aqueous $SrCl_2$ from 295 K to 625 K at p = 20 MPa: ♦, 296 K; ●, 376 K.; □, 446 K; ▲, 502 K; △, 549 K; ◇, 600 K; ○, 625 K; plain line, TBBK fit.
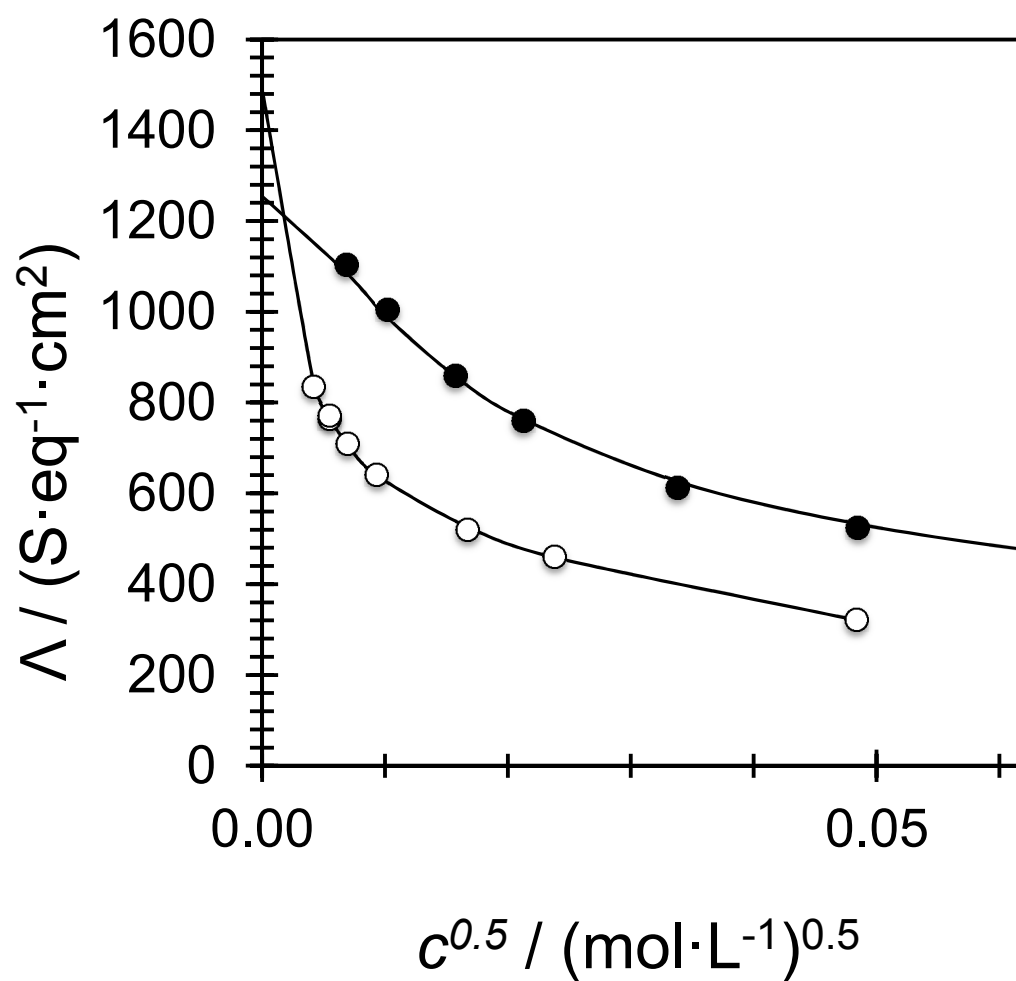
Figure 3. Experimental equivalent conductivities of aqueous $Sr(OH)_2$, $\bigcirc$, and aqueous $SrCl_2$, $\bullet$, at $T =$ 625 K and $p = 20$ MPa. Plain lines represent TBBK fits.
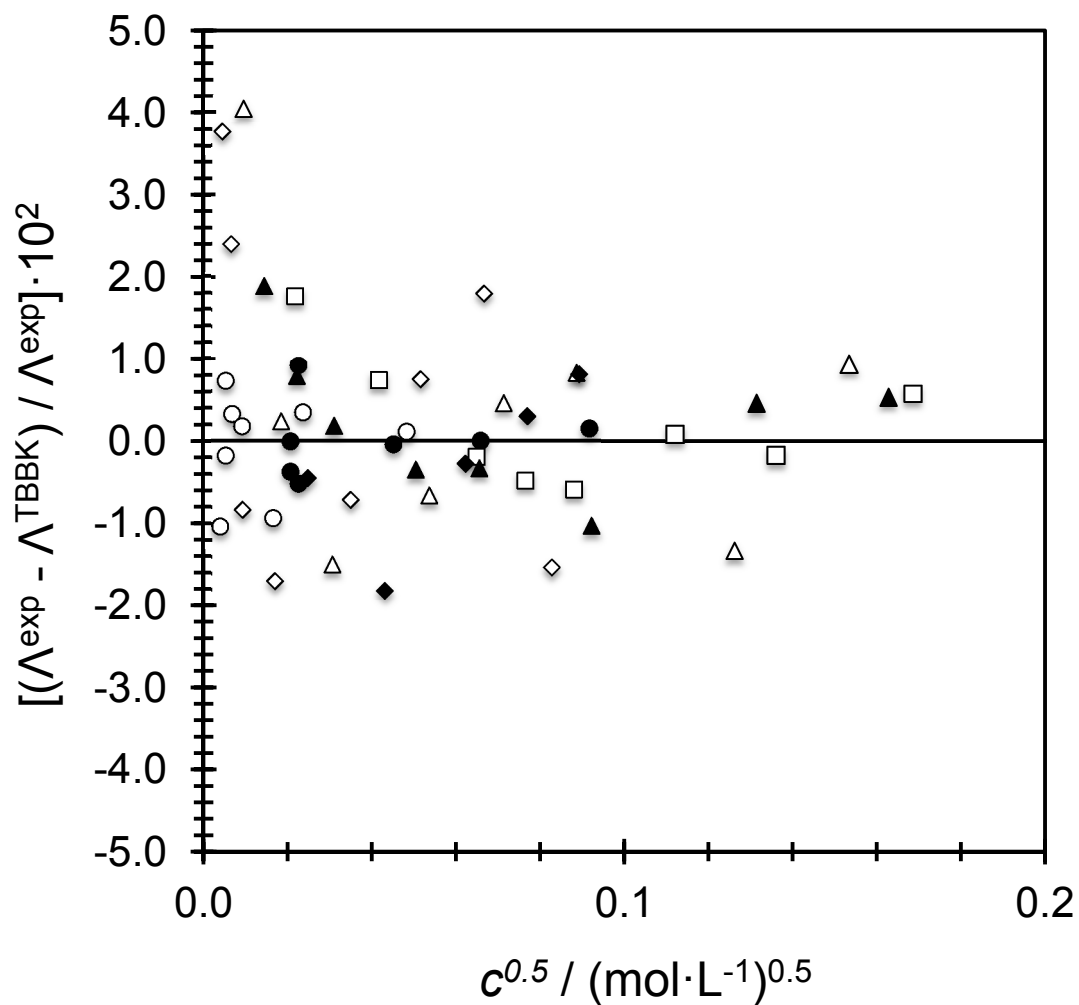
Figure 4.a. Percent difference of the residuals versus the square root of the concentration of $Sr(OH)_2$ from 295 K to 625 K at $p = 20$ MPa when fitting with the TBBK equation: $\diamondsuit$, 295 K; $\bigcirc$, 375 K; $\square$, 447 K; $\triangle$, 502 K; $\blacklozenge$, 548 K; $\blacktriangle$, 599 K; $\bullet$, 625 K.
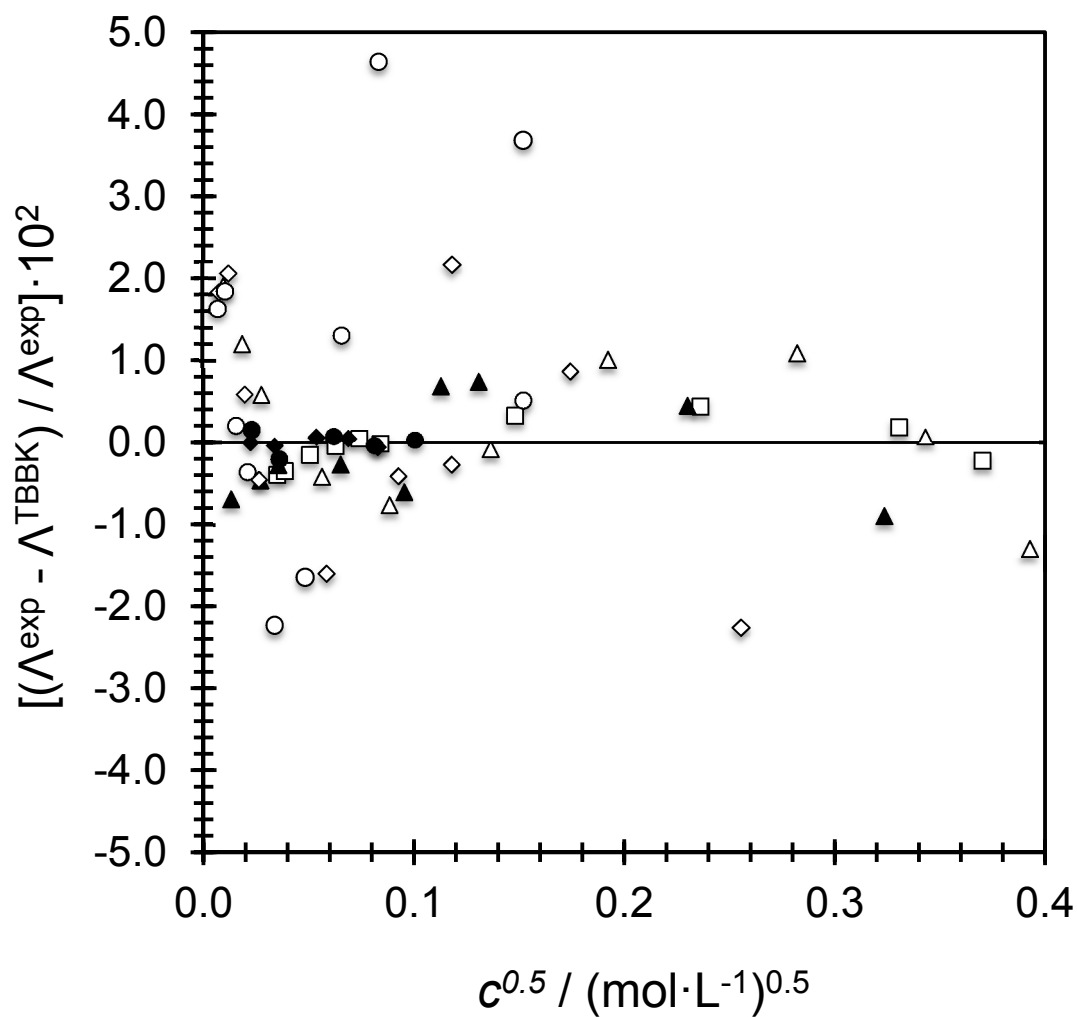
Figure 4.b. Percent difference of the residuals versus the square root of the concentration of $SrCl_2$ from 295 K to 625 K at p = 20 MPa when fitting with the TBBK equation: $\diamond$, 296 K; $\bigcirc$, 376 K; $\square$, 446 K; $\triangle$, 502 K; $\blacklozenge$, 549 K; $\blacktriangle$, 600 K; $\bullet$, 625 K.
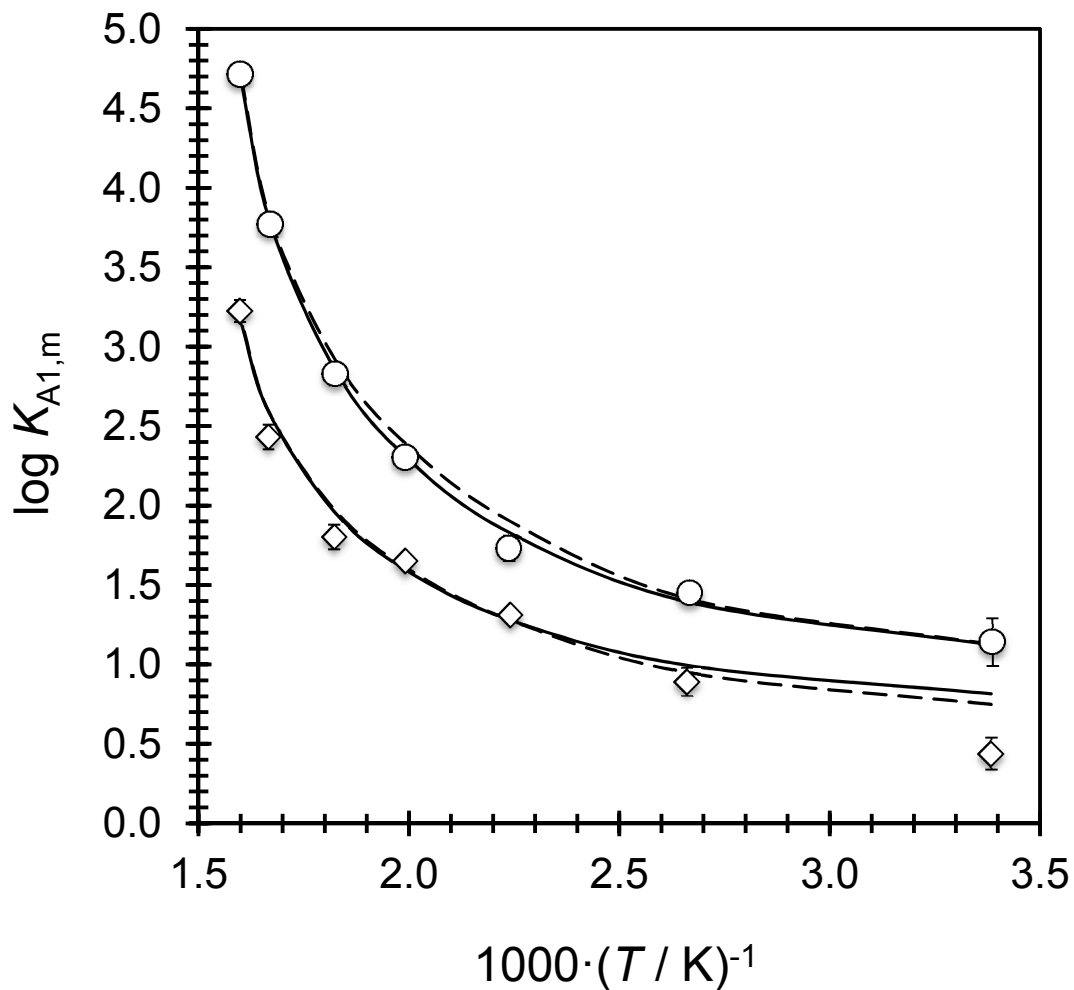
Figure 5. Experimental values for the first association constants of Sr(OH)$_2$ and SrCl$_2$ in H$_2$O from 295 K to 625 K at p = 20 MPa derived from the TBBK equation: $\bigcirc$, Sr^{2+} + OH$^-$ $\leftrightarrows$ Sr(OH)$^+$; $\diamondsuit$, Sr^{2+} + Cl$^-$ $\leftrightarrows$ SrCl$^+$; plain lines, density model fit #1 (eq 14); dashed line, density model fit #2 (eq 14).

47
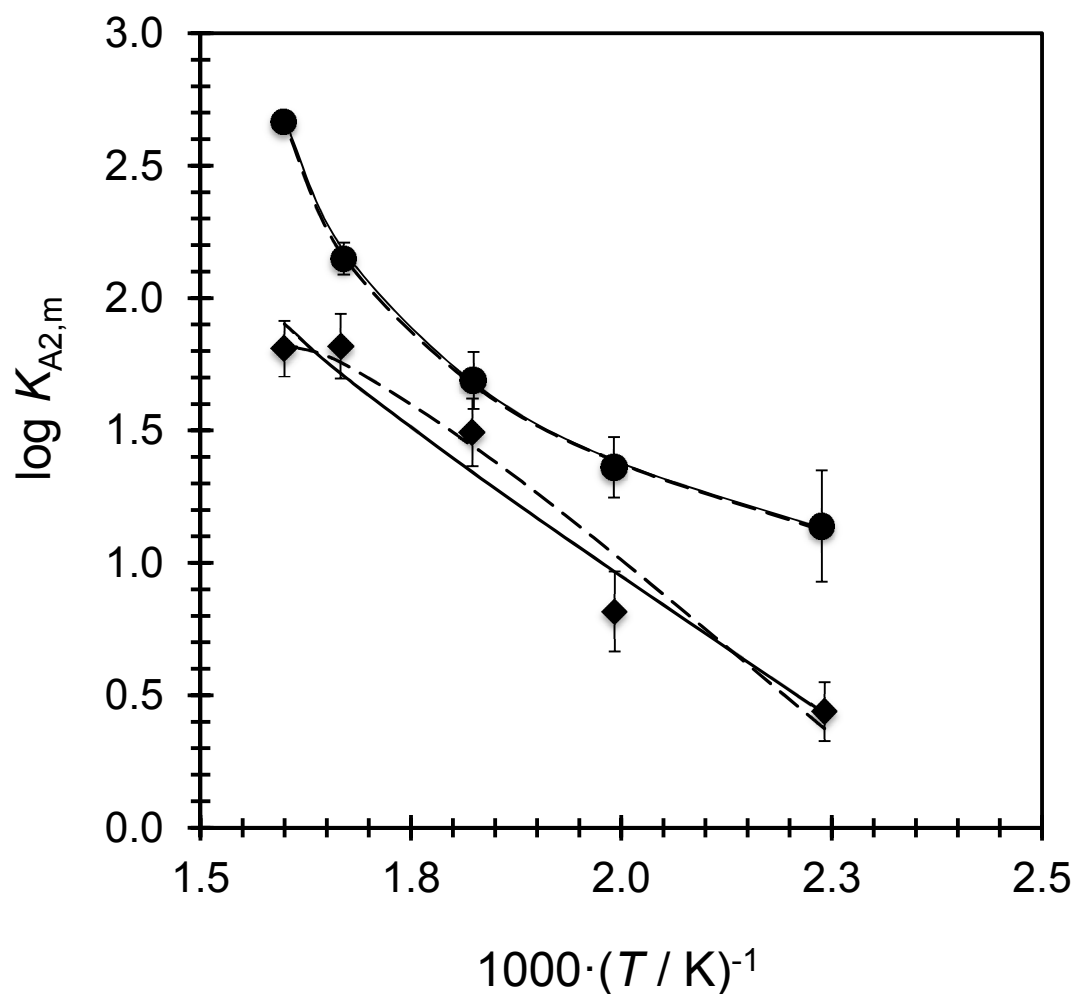
Figure 6. Experimental values for the second association constants of $Sr(OH)_2$ and $SrCl_2$ in H_2O from 295 K to 625 K at p = 20 MPa derived from the TBBK equation: ●, $Sr(OH)^+$ + $OH^- \leftrightarrows Sr(OH)_2^0$; ◆, $SrCl^+$ + $Cl^- \leftrightarrows SrCl_2^0$; plain lines, density model fit #1 (eq 14); dashed line, density model fit #2 (eq 14).
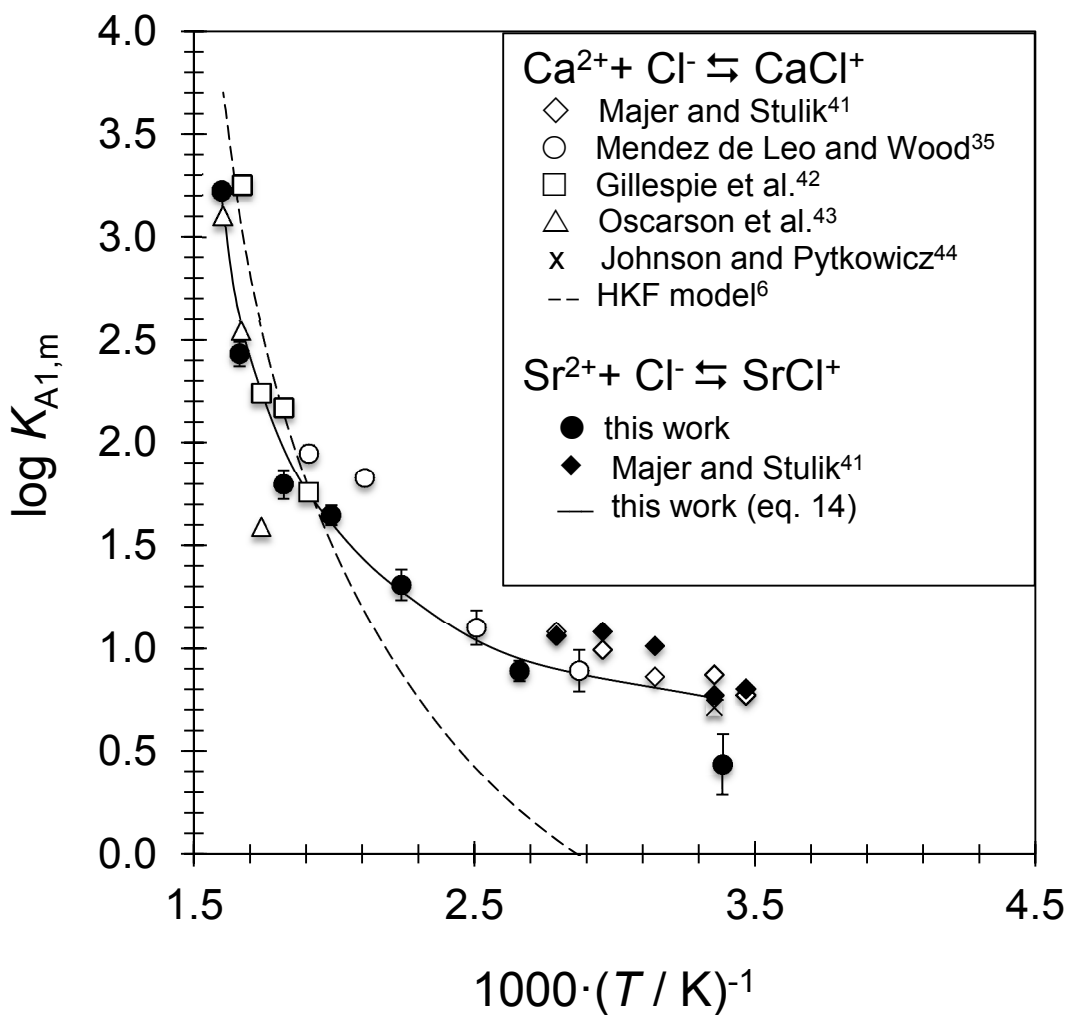
Figure 7. Comparison between calcium and strontium chloride first association constants as a function of temperature. $Ca^{2+} + Cl^- \leftrightarrows CaCl^+$: $\diamondsuit$, Majer and Stulik[41] corrected values; $\bigcirc$, Mendez de Leo and Wood[35]; $\square$, Gillespie et al.[42]; $\triangle$, Oscarson et al.[43]; X, Johnson and Pytkowicz[44]; --, HKF model[6]. $Sr^{2+} + Cl^- \leftrightarrows SrCl^+$: $\bullet$, this work; $\blacklozenge$, Majer and Stulik[41] corrected values; $-$, eq 14.

$$R_{298}^{T} = \frac{(\lambda^{\circ}\eta_w)_T}{(\lambda^{\circ}\eta_w)_{T=298\ K}}$$

$$R_{298}^{T} = \frac{(\lambda^{\circ}\eta_w)_T}{(\lambda^{\circ}\eta_w)_{T=298\ K}}$$
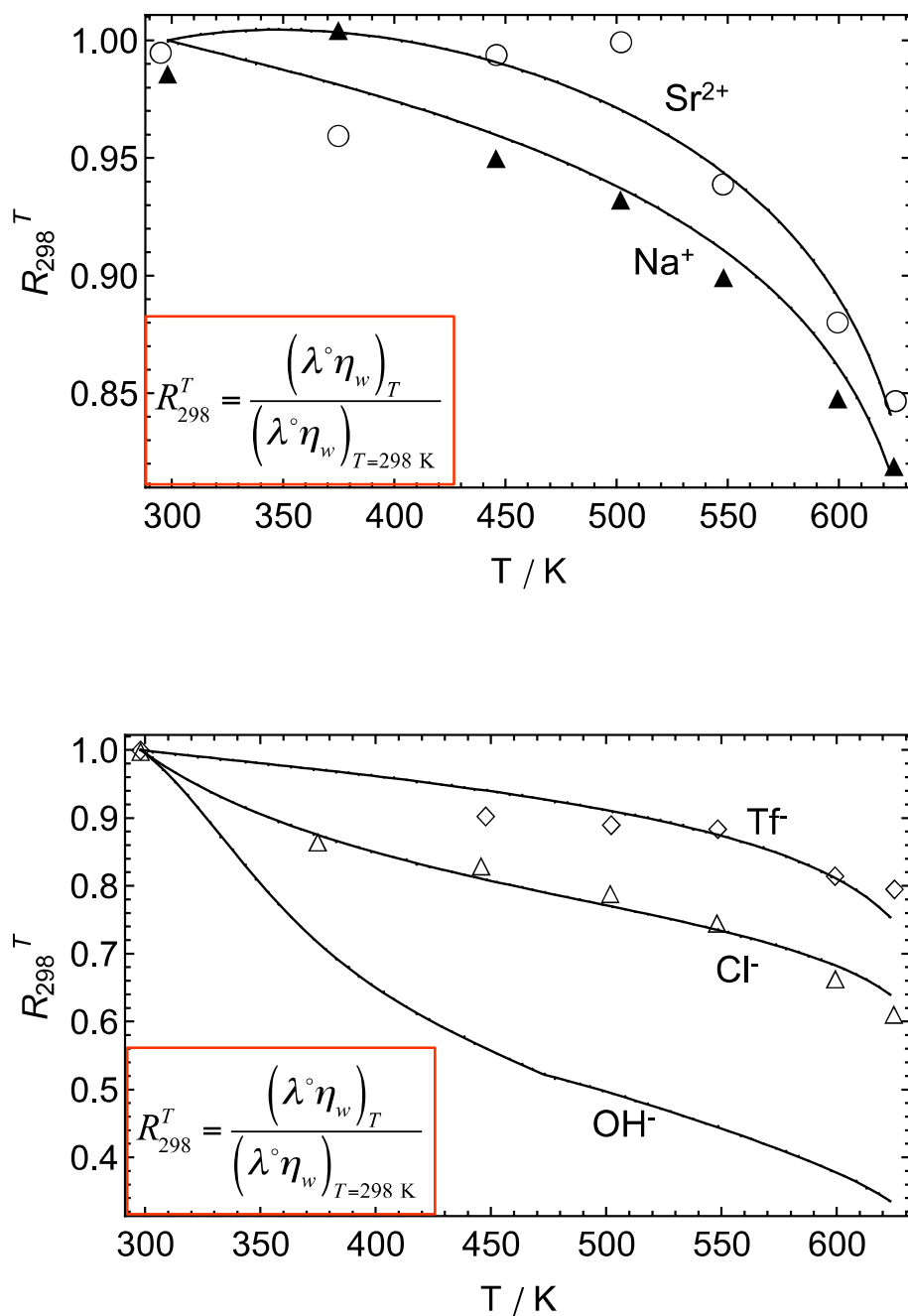
Figure 8. Temperature dependence of the Walden product ratio for aqueous anions and cations relevant to this work, from The values for the limiting single ion conductivity, λ°, were taken from Zimmerman et al.,[16,18] Ho et al.,[37] and Marshall.[36]
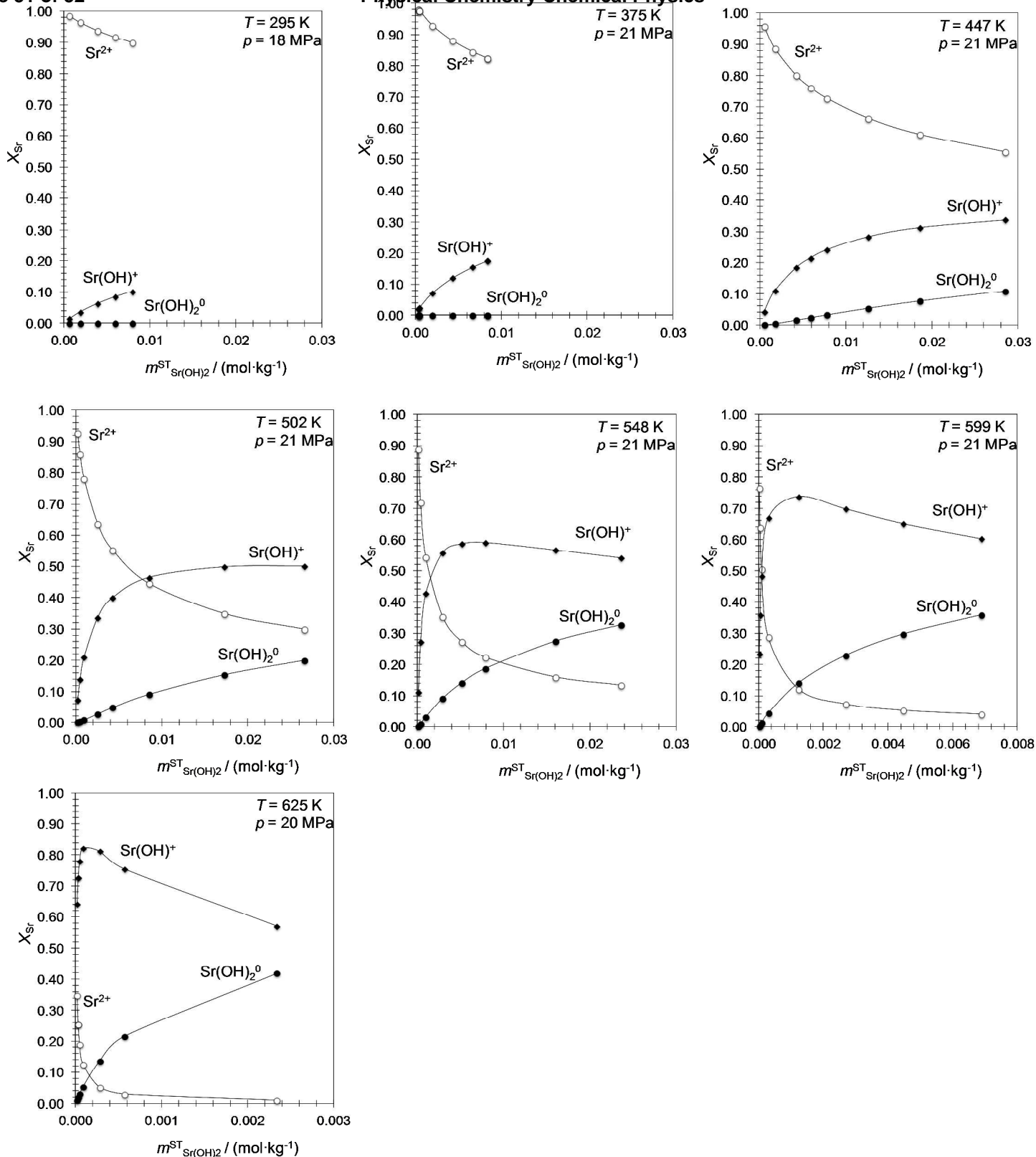
Figure 9. Distribution of species in aqueous $Sr(OH)_2$ as a function of the stoichiometric concentration from $T = 295$ K to 625 K and $p \sim 20$ MPa: $\bigcirc$, Sr^{2+} (free cation); $\blacklozenge$, $Sr(OH)^+$ (charged ion pair); $\bullet$, $Sr(OH)_2^0$ (neutral ion pair).
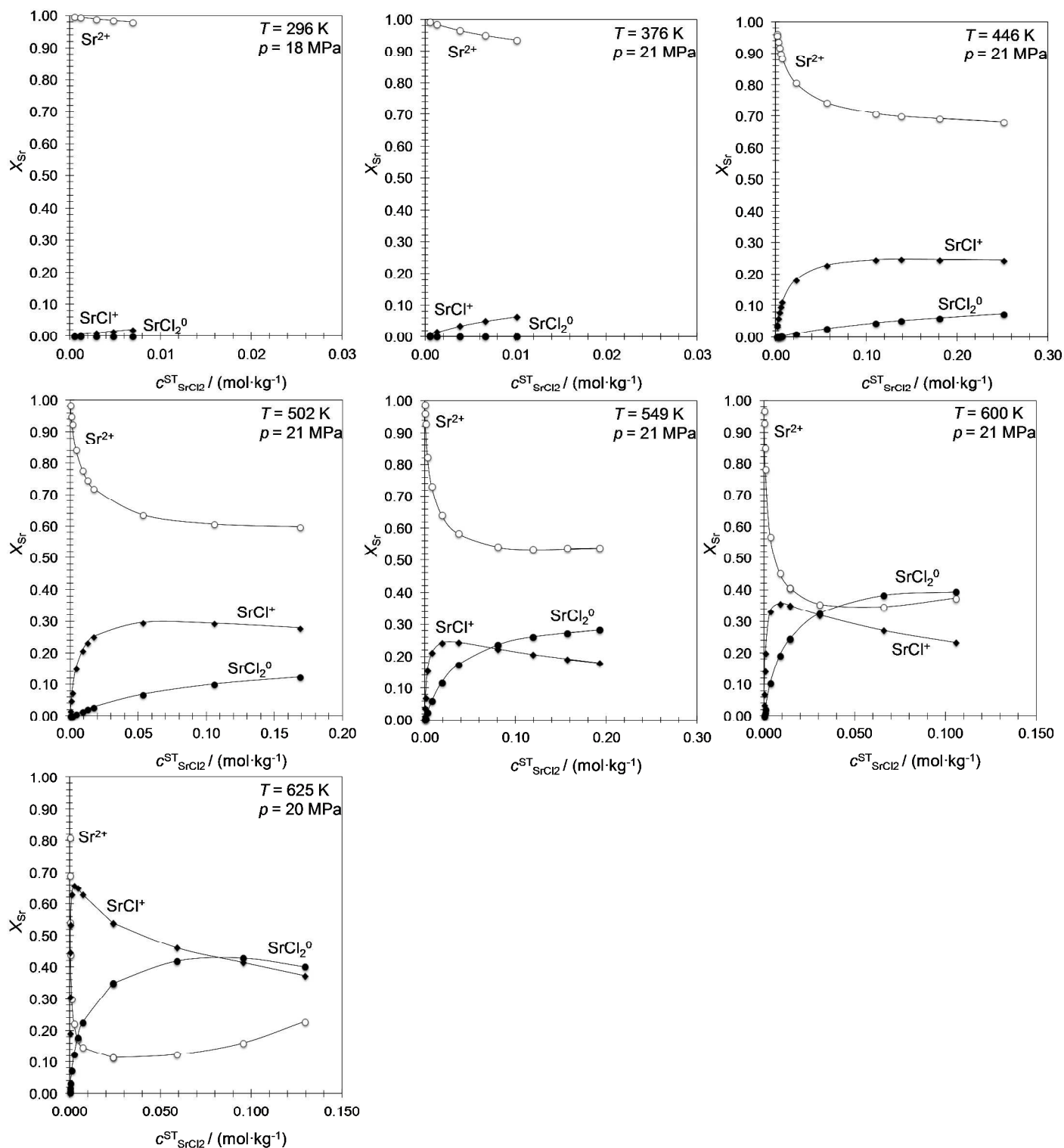
Figure 10. Distribution of species in aqueous $SrCl_2$ as a function of the stoichiometric concentration from T = 295 K to 625 K and p ~ 20MPa: $\bigcirc$, Sr^{2+} (free cation); $\blacklozenge$, $SrCl^+$ (charged ion pair); $\bullet$, $SrCl_2^0$ (neutral ion pair).